



Published in final edited form as:

Respir Physiol Neurobiol. 2022 May ; 299: 103855. doi:10.1016/j.resp.2022.103855.

Contribution of the Caudal Medullary Raphe to opioid induced respiratory depression

Barbara Palkovic, MD^{1,2}, Denise Cook-Snyder, PhD^{1,3,4}, Jennifer J. Callison, BS¹, Thomas M. Langer 3rd, MD, PhD¹, Riley Nugent^{1,5}, Eckehard A.E. Stuth, MD^{1,6}, Edward J. Zuperku, PhD^{1,7}, Astrid G. Stucke, MD^{1,6}

¹:Department of Anesthesiology, Medical College of Wisconsin, Milwaukee, WI

²:Faculty of Medicine, University of Osijek, Osijek, Croatia

³:Department of Neuroscience, Carthage College, Kenosha, WI

⁴:Department of Physiology, Medical College of Wisconsin, Milwaukee, WI

⁵:Carroll University, Waukesha, WI

⁶:Children's Wisconsin, Milwaukee, Wisconsin

⁷:Zablocki VA Medical Center, Milwaukee, Wisconsin

Abstract

Background: Opioid-induced respiratory depression can be partially antagonized in the preBötzing Complex and Parabrachial Nucleus/Kölliker-Fuse Complex. We hypothesized that additional opioid antagonism in the caudal medullary raphe completely reverses the opioid effect.

Methods: In adult ventilated, vagotomized, decerebrate rabbits, we administered remifentanyl intravenously at “analgesic”, “apneic”, and “very high” doses and determined the reversal with sequential naloxone microinjections into the bilateral Parabrachial Nucleus/Kölliker-Fuse Complex, preBötzing Complex, and caudal medullary raphe. In separate animals, we injected opioid antagonists into the raphe without intravenous remifentanyl.

Results: Sequential naloxone microinjections *completely* reversed respiratory rate depression from “analgesic” and “apneic” remifentanyl, but not “very high” remifentanyl concentrations. Antagonist injection into the caudal medullary raphe without remifentanyl independently increased respiratory rate.

Corresponding author: Astrid G. Stucke, MD, Department of Anesthesiology, Medical College of Wisconsin, 9200 W Wisconsin Ave, Milwaukee, WI, 53226, Phone: 414-266-3560, astucke@mcw.edu.

Publisher's Disclaimer: This is a PDF file of an unedited manuscript that has been accepted for publication. As a service to our customers we are providing this early version of the manuscript. The manuscript will undergo copyediting, typesetting, and review of the resulting proof before it is published in its final form. Please note that during the production process errors may be discovered which could affect the content, and all legal disclaimers that apply to the journal pertain.

Prior presentations: This work was presented in part at the annual Experimental Biology meeting, virtual meeting, April 27–30, 2020 and the annual meeting of the American Society of Anesthesiologists, San Diego, October 8–12, 2021.

Conflicts of interest: The authors declare no competing interests.

Conclusions: Opioid-induced respiratory depression results from a combined effect on the respiratory rhythm generator and respiratory drive. The effect in the caudal medullary raphe is complex as we also observed local antagonism of endogenous opioid receptor activation, which has not been described before.

Keywords

Parabrachial Nucleus/ Kölliker-Fuse Complex; preBötzinger Complex; Caudal Medullary Raphe; Opioid-induced respiratory depression; Respiratory phase timing; Respiratory rhythm generator

Introduction

Multiple *in vivo* studies have demonstrated that a significant part of opioid-induced respiratory depression at analgesic opioid concentrations is due to depression of the respiratory rhythm generator in the preBötzinger Complex as well as the Parabrachial Nucleus/Kölliker-Fuse Complex (PBN/KF), which provides inputs to the preBötzinger Complex (1–8). Two studies in decerebrate rabbits (1) and freely behaving mice (4) highlighted that restoring neuronal activity in the PBN/KF and preBötzinger Complex through either localized naloxone injections (1) or localized mu-opioid receptor deletion (4) had more limited reversal effects at higher opioid doses. This implied opioid-induced depression of *respiratory drive* to these areas. Chemosensitive neurons in the retrotrapezoid nucleus, the main source and integrator of chemodrive in the brainstem (9), were not affected by apneic doses of morphine (10). However, injection of the mu-opioid receptor antagonist D-Phe-Cys-Tyr-D-Trp-Arg-Thr-Pen-Thr-NH₂ (CTAP) into the caudal medullary raphe, another part of the chemoreceptive system, partially reduced a moderate respiratory rate depression (~30%) from intravenous [D-Ala,²N-MePhe,⁴Gly-ol]-enkephalin (DAMGO) in rats *in vivo* (11). Phillips et al. showed that naltrexone injection into the rostral ventromedial medulla, i.e., the raphe at the caudal pole of the facial nucleus, reversed the respiratory depression and analgesia from analgesic doses of intravenous morphine (12). The maximal effect occurred 20 minutes after injection, suggesting that diffusion was necessary to sufficiently antagonize the affected neuronal population (12). Neither study injected the opioid antagonist without systemic opioids (11, 12).

We hypothesized that injection of the opioid antagonist naloxone into the caudal medullary raphe in addition to the PBN/KF and preBötzinger Complex would completely reverse opioid-induced respiratory depression from “analgesic”, “apneic”, and “very high” remifentanyl concentrations. We also injected naloxone into the caudal medullary raphe without systemic remifentanyl to rule out endogenous opioid receptor activation. We found a substantial increase in respiratory rate, which prompted us to repeat the protocol without systemic remifentanyl with local injections of more specific mu- and delta-opioid receptor agonists. Last, we determined whether the endogenous opioid ligand maximally activated the raphe opioid receptors with additional localized DAMGO microinjection.

Methods

2.1. Surgical preparation

The research was approved by the Institutional Animal Care and Use Committee, Medical College of Wisconsin, in accordance with provisions of the Animal Welfare Act, and the Public Health Service Guide for the Care and Use of Laboratory Animals. Experiments were carried out on adult (3–4 kg) New Zealand White rabbits of either sex. The preparation has been previously described in detail(1). In short, animals were anesthetized and ventilated via tracheotomy with an anesthesia machine (Ohmeda CD, GE, Datex Ohmeda, Madison, WI). Inspiratory oxygen fraction, expiratory carbon dioxide concentration and expiratory isoflurane concentration were continuously displayed with an infrared analyzer (POET II, Criticare Systems, Waukesha, WI). Femoral arterial and venous lines were used for blood pressure monitoring, infusion of solutions, and bolus drug application, respectively. Lactated Ringer's solution with 3 mcg/ml epinephrine was continuously infused at 1 ml/h, and rate was increased as needed to counteract or prevent hypotension in response to drug injections and/or from blood loss. The animal was maintained at $37.0 \pm 0.5^{\circ}\text{C}$ with a warming blanket. The animal was placed in a stereotaxic frame (David Kopf Instruments, Tujunga, CA). After blunt precollicular decerebration, isoflurane was continued at subanesthetic levels (0.3–0.4 vol%) for blood pressure control, and animals were paralyzed with rocuronium (15 mg/kg subcutaneous bolus), followed by pancuronium or vecuronium (2 mg/h) infusion to avoid motion artifacts during neural/neuronal recording. The brainstem was exposed via occipital craniotomy and partial removal of the cerebellum. Bilateral vagotomy was performed to achieve peripheral deafferentation. The phrenic nerve was recorded with fine bipolar electrodes through a posterior neck incision. The complete surgical preparation required 6–7h. Throughout the experiment animals were ventilated with hyperoxia (FiO_2 0.6) and maintained at mild hypercapnia (expiratory carbon dioxide: 45–55 mmHg). Blood pressure was maintained stable throughout the protocols by adjusting the intravenous infusion rate. At the end of the experiment, animals were euthanized with intravenous potassium chloride.

2.2. Neuronal Recording, microinjection procedures and measured variables

All neuronal recording and microinjection techniques have been well established by our research group and have been previously described in detail (1, 13, 14). In short, extracellular neuronal recordings were obtained using multibarrel micropipettes (20–40 μm tip diameter) consisting of three drug barrels and a recording barrel containing a 7 μm thick carbon filament. Barrels were filled with the glutamatergic agonist α -amino-3-hydroxy-5-methyl-4-isoxazolepropionic acid (AMPA, 50 μM , 70 nl/ injection) and the opioid receptor antagonist naloxone (1mM, 700nl/injection), which were dissolved in artificial cerebrospinal fluid (aCSF). The microinjected volume was determined via height changes in the meniscus in the respective pipette barrel with a 100x monocular microscope and calibrated reticule (resolution ~ 3.5 nl). Respiratory neuronal discharge was recorded extracellularly and classified by the temporal relationship relative to the phrenic neurogram. Neuronal discharge rate-meter, pressure microejection marker signals, phrenic neurogram, respiratory rate, arterial blood pressure, and airway carbon dioxide concentration were continuously displayed and recorded using a digital acquisition system (Powerlab/16SP; ADInstruments, Castle Hill, Australia). Before and after drug injection, steady-state conditions were obtained

for respiratory parameters. Post experiment LabChart data was exported to SigmaPlot 11 (Systat Software, San Jose, CA) for data reduction, data plotting and statistical analysis. Between 10 and 50 consecutive respiratory cycles were averaged over 1–2 min with the number of cycles dependent on the respiratory rate. Using the phrenic neurogram we determined respiratory rate, inspiratory and expiratory duration, and peak phrenic activity. Peak phrenic activity was normalized to control values for all calculations (15).

2.3. Functional identification of the Parabrachial Nucleus/ Kölliker-Fuse complex, preBötzinger complex, and caudal medullary raphe

As previously described, we identified the locations of the parabrachial nucleus/ Kölliker-Fuse complex (PBN/KF) (16) and preBötzinger Complex (1, 14) bilaterally through stereotaxic coordinates, neuronal recordings and typical respiratory rate response to AMPA microinjection (50 μ M, 70nl). For the current study, we first identified the preBötzinger Complex, which was on average 2.3 ± 0.1 mm rostral to obex, 2.7 ± 0.1 mm lateral from midline, and 4.8 ± 0.1 mm ventral to the dorsal surface (n=52). We then identified the PBN, which was on average 9.6 ± 0.1 mm rostral to the preBötzinger Complex, 2.7 ± 0.1 mm lateral to midline and 8.7 ± 0.1 mm ventral to the dorsal surface (n=40). The distance between preBötzinger Complex and PBN was remarkably consistent, and both areas were at the same lateral distance from midline, which facilitated the functional identification. Based on our previous studies that showed a consistent distance between PBN and KF (1, 16), we used the location 0.94mm caudal (1mm, corrected for the 20° - angle on the stereotaxic frame), 0.5mm lateral, and 2mm ventral to the PBN for study drug injections into the KF without additional AMPA mapping. Complete, bilateral functional identification of all areas including the time required for respiratory rate to return to baseline after each AMPA injection required 4–5h.

To determine the location of the caudal medullary raphe, we performed a pilot study in six animals using grid-wise injections of AMPA into the midline between 3mm caudal and up to 7mm rostral to the functionally identified preBötzinger Complex with step size 0.47mm (0.5mm rostro-caudal, corrected for the 20° - angle of the stereotaxic frame). We microinjected AMPA (50 μ M, 70nl) starting at the ventral limit of the tonic neuronal activity and then in 0.5 mm steps more dorsally. Due to the long duration of the AMPA effect and the multiple injections per coordinate, mapping was performed for the raphe caudal to the preBötzinger Complex in three animals and rostral to the preBötzinger Complex in three different animals. The rostro-caudal level of the preBötzinger Complex was identified in all animals. Changes in respiratory activity in % baseline were averaged for coordinates relative to obex and, alternatively, relative to the functionally identified preBötzinger Complex. We found that AMPA effects were more consistent between animals when the coordinates were compared relative to the preBötzinger Complex. Figure 1 shows the averaged values relative to the preBötzinger Complex, with the preBötzinger Complex level pictured at 2.5mm rostral to obex. AMPA injections caudal to the preBötzinger Complex level consistently increased respiratory rate and peak phrenic activity. The onset of the effect was more delayed than AMPA effects in, e.g., the preBötzinger Complex or Parabrachial Nucleus (1) (fig.1A). We also observed tachypnea after AMPA injection into the nucleus of the solitary tract (NTS), however, the effect occurred immediately after AMPA injection, and in

each animal, there was a rostro-caudal gap of 0.5–1mm between the location of immediate tachypnea (NTS) and the delayed tachypnea observed in the raphe. Although in one animal AMPA injections rostral to the preBötzing Complex decreased respiratory rate and peak phrenic activity resulting in an average decrease (fig.1C), in other animals we observed an increase respiratory rate and peak phrenic activity up to 1.5 mm rostral to the preBötzing Complex level. The most severe depression of respiratory rate and peak phrenic activity was observed at >3mm rostral to the preBötzing Complex level, i.e., at the level of the caudal pole of the facial nucleus, where AMPA injection could cause complete apnea (17). Based on the distribution of the tachypneic response, for all opioid protocols, drug injections into the caudal medullary raphe were performed between 2mm caudal and 1.5mm rostral to the preBötzing Complex level.

2.4. Histology

Histological confirmation of the caudal medullary raphe area was obtained in a separate group of animals to minimize tissue damage from the electrode. In our standard in vivo preparation, the bilateral location of the preBötzing Complex was functionally identified with AMPA injection. Fluorescent latex microspheres (140nl, [Lumafly.com](https://www.lumafly.com/); Red Retrobeads), diluted to 5% of the supplied concentration, were microinjected into the bilateral preBötzing Complex and at the coordinates where functional identification had suggested the caudal end of the caudal medullary raphe (i.e., midline, 2mm caudal to the preBötzing Complex and at the ventral limit of recorded neuronal activity) and the rostral medullary raphe (17, 18)/ rostral ventromedial medulla (12) (i.e., midline, 3mm rostral to the preBötzing Complex and at the ventral limit of recorded neuronal activity). Animals were transcardially perfused with phosphate-buffered saline and paraformaldehyde (4%), and the brainstem was submersed in paraformaldehyde for 5 days and stored in hypertonic sucrose (30% in PBS) with sodium azide (0.1%) before being flash frozen in isopentane and sectioned using a cryostat (Leica). Sequential 20µm coronal sections were cut from the caudal edge of the inferior colliculi to 2mm caudal to obex. Immunolabeling of free-floating sections was performed as previously described (14, 16) using goat anti-ChAT (1:100, Millipore Cat# AB144P, RRID:AB_2079751), or goat anti-5HT (1:1000, ImmunoStar Cat# 20079, RRID:AB_572262) on consecutive sections, and donkey anti-goat Alexa Fluor 488 (1:500, Jackson ImmunoResearch Labs Cat# 705-545-147, RRID:AB_2336933) on all sections. The immunohistochemical staining patterns obtained with the antibodies was in agreement with the known expression patterns of the corresponding proteins, both at the cellular and subcellular level, supporting the specificity of these antibodies. Sections were counterstained with DAPI dihydrochloride (0.5µg/ml, Invitrogen Cat# D1306) for 5min at room temperature then mounted to glass slides using Fluoromount-G (Southern Biotech), coverslipped, and stored at 4 ° C until imaging. An inverted fluorescence slide scanning microscope (Keyence BZ-X810) at a 20x objective was used for all image acquisition. The resolution and exposure settings were identical between experimental groups. The atlas of Meessen and Olszewski (19) and a later study by Felten and Cummings (20) were used for identification of relevant regions. Fig.2 illustrates the anatomical reference points, e.g., obex, preBötzing Complex and facial nucleus, that confirm the location of the caudal medullary raphe, which based on functional identification (2.3.) is located between 2mm caudal to the preBötzing Complex (near obex) to 1.5mm rostral to the preBötzing Complex, i.e.,

halfway between preBötzinger Complex and the caudal end of the facial nucleus in our preparation.

2.5. Opioid effect sites at “analgesic” IV remifentanil concentrations

Experimenters were not blinded to the experimental conditions, and we did not perform formal randomization to experimental protocols. Since the effect of naloxone microinjection persists >2h, only one complete protocol was performed per animal. Protocols investigating “analgesic”, “apneic”, and “very high” concentrations were performed in the same animals as illustrated in fig.3. Thus the observed opioid and naloxone effects could be compared against the same initial baseline respiratory rate. Great care was taken to await complete recovery from opioid bolus injections (2.6.) to the respiratory rate present before the bolus before continuing with the naloxone microinjection protocol. Testing multiple remifentanil concentrations in the same animal also allowed verification that the naloxone injection sites were correct, e.g., when a “very high” remifentanil bolus (2.7.) still caused significant respiratory depression but the naloxone injections had reversed the effects of “analgesic” and “apneic” remifentanil concentrations comparably to the other animals. At the end of the experiments, naloxone 20–40 mcg/kg was injected intravenously to document that respiratory rate returned to the pre-remifentanil control. Only thereafter was the remifentanil infusion discontinued. For ease of reading, the different opioid concentrations are presented separately.

To determine how much opioid effects in the PBN/KF, preBötzinger Complex, and caudal medullary raphe contributed to systemic opioid-induced respiratory depression at “analgesic” opioid doses, we infused remifentanil intravenously at an average of 0.16 ± 0.06 mcg/kg/min until respiratory rate was depressed by approximately 50% (fig.3). The choice of opioid (21, 22) and dose (23, 24) have been discussed before (1). Cohort A: After reaching steady-state effect for 10–15 min, naloxone (1mM, 700nl) (1, 14, 16) was microinjected bilaterally into the Kölliker-Fuse Nucleus, the Parabrachial Nucleus, and the preBötzinger Complex. At least 5 min were allowed after each injection site to obtain maximal effect. We recently reported that our standard approach, i.e., a single injection into the bilateral, functionally identified preBötzinger Complex did not completely reverse the opioid effect in all animals, but that additional injections into the rostral ventral respiratory group caused an additional reversal of respiratory rate depression by 1 (0–3) breath per minute (bpm) (1). To ensure complete reversal of the rhythm generating area, in the current study we also injected naloxone bilaterally into the premotor neuron area (14), i.e., at 0.5mm caudal to the preBötzinger Complex/ same depth, at 1 mm caudal and 1mm dorsal to the preBötzinger Complex, and at 1.5mm caudal, 0.5mm medial, and 1.5mm dorsal to the preBötzinger Complex. For the entire study, the term “preBötzinger Complex injection” includes injections into the premotor neuron area. Subsequently, we microinjected naloxone (1mM) into the caudal medullary raphe, moving in 0.5mm increments between 2mm caudal and 1.5mm rostral to the preBötzinger Complex level. To ensure that naloxone injections covered the raphe pallidus as well as obscurus but did not diffuse too far lateral, we injected 350nl at the ventral limit of neuronal activity and another 350nl at 2mm dorsal to the first injection. We waited for steady-state effect after injections into the area caudal to, at the level of, and rostral to the preBötzinger Complex to evaluate

whether the naloxone effect was limited to any subarea of the caudal medullary raphe. Initial analysis showed an additional naloxone effect in each subarea, and we used the values at the end of the entire caudal medullary raphe injection sequence for the statistical analysis. **Cohort B:** To determine whether the order of naloxone injections, i.e., pons to raphe, determined the magnitude of reversal in the individual brainstem nuclei, in a second set of animals we injected naloxone starting with the caudal medullary raphe, followed by the preBötzing Complex, and finally the PBN/KF. **Cohort C:** In a third group of animals, we injected naloxone only into the preBötzing Complex and caudal medullary raphe to evaluate whether prior reversal of the PBN/KF affected the magnitude of the naloxone reversal in the caudal medullary raphe. Interim analysis after five animals showed that naloxone injection into the caudal medullary raphe had very similar effects on inputs to inspiratory off-switch (after PBN/KF+preBötzing Complex reversal: 22 (19–28)% vs. after preBötzing Complex reversal only 25 (12–58)%) and inspiratory on-switch (26 (19–28)% vs. 22 (2–27)%). Since the overall focus of the study was the effect of combined naloxone reversal in the PBN/KF, preBötzing Complex, and caudal medullary raphe, we stopped data acquisition for Cohort C after five animals to reduce animal use. Available data are presented. Data are included in the subanalysis of inputs to respiratory phase switch (see Results 3.6.) and additional effects of naloxone injection into the premotor neuron area, compared to the preBötzing Complex (see additional analysis, Results 3.1. and 3.2.).

2.6. Opioid effect sites at “apneic” IV remifentanil concentrations

To determine whether the contributions of the PBN/KF, preBötzing Complex, and caudal medullary raphe to opioid-induced respiratory depression varied with different systemic opioid concentrations, we injected an intravenous remifentanil bolus that was sufficient to cause apnea >60sec (average 12 ± 2 mcg) (fig.3) as described before (1). The dose necessary to achieve apnea was determined for each individual animal and the individualized dose was used as the “apneic bolus” throughout the entire experiment. In **Cohort A**, the “apneic” bolus was repeated after naloxone injection into the PBN/KF plus preBötzing Complex and third after naloxone injection into the caudal medullary raphe. In **Cohort B**, the “apneic” bolus was repeated after naloxone injection into the caudal medullary raphe and third after naloxone injection into the preBötzing Complex plus PBN/KF. In **Cohort C**, the “apneic” bolus was repeated after naloxone injection into the preBötzing Complex and third after naloxone injection into the caudal medullary raphe. As described above, we stopped data acquisition for this cohort after interim analysis.

2.7. Effects of “very high” remifentanil concentrations on areas outside the Parabrachial Nucleus/Kölliker-Fuse Complex, preBötzing Complex, and Caudal Medullary Raphe

We investigated whether “very high” remifentanil doses depressed respiration after naloxone injection into the PBN/KF, preBötzing Complex, and caudal medullary raphe, which would point to depression of additional areas providing respiratory drive or controlling the respiratory motor output. After complete recovery of respiratory rate from the third “apneic” remifentanil bolus we injected intravenous remifentanil in 10–50 mcg increments until apnea or a maximum dose of 100mcg. Injections were staggered in short sequence to avoid arterial hypotension, but the maximal dose was generally administered within 2–3

min. The entire experiment including surgical preparation, functional identification of the injection sites and the remifentanyl/ naloxone protocol required 18–20h.

2.8. Effects of naloxone, CTAP and naltrindole, and aCSF in respiratory premotor neurons and the caudal medullary raphe

We have previously described that naloxone and aCSF injections into the PBN/KF or preBötzing Complex did not have any independent effects on respiration suggesting lack of endogenous opioid receptor activation in these areas (1). To confirm that the effect of local naloxone microinjections we observed during remifentanyl infusion represented a reversal of the exogenous, intravenous remifentanyl effect we injected naloxone (1mM, 350nl) into the premotor neurons and into the caudal medullary raphe as described in the above protocols in the absence of remifentanyl. However, since we unexpectedly found a consistent increase in respiratory rate with naloxone injections into the caudal medullary raphe, which suggested endogenous opioid receptor activation, we repeated the injection protocols in the raphe without remifentanyl in a separate group of animals with the specific mu-opioid receptor agonist CTAP (1mM, 350nl) and the delta-receptor antagonist naltrindole (1mM, 350nl). As a control, we also injected aCSF (350nl), which was used as solvent for all injected drugs, into the caudal medullary raphe to rule out an independent vehicle effect.

2.9. Effects of high concentrations of DAMGO in the caudal medullary raphe

To determine whether endogenous ligands maximally activated opioid receptors in the caudal medullary raphe, we injected DAMGO (200µM, 350nl) into the caudal medullary raphe as described in the above protocols. At the end of the injection sequence, the effect was reversed with intravenous naloxone (20 mcg/kg).

2.10. Statistical analysis

Statistical analysis was performed using SigmaPlot 11 (Systat Software, USA). We did not perform a formal power analysis, and no adjustments were made for interim analyses. Comparable studies have used 4 to 9 rats (3) ((25), 4 to 11 mice (4, 5), 8 to 16 rabbits (1, 6, 26), and 10 to 21 dogs (7, 27) per protocol.

Since experiments were technically very difficult and labor intensive, we included data from a few animals where one single data point was missing. The total number of animals is indicated for each comparison. To eliminate the problem of “missing values” and data with boundaries (apnea), we calculated the difference (“delta”) for each variable between naloxone injections and IV remifentanyl, or between sequential naloxone injections into the areas of interest as described before (1) and detailed in the Results. Testing revealed that not all “deltas” were normally distributed (Shapiro-Wilk test). For paired data, we uniformly used the Wilcoxon Signed Rank test to test each “delta” against no change (Null-Hypothesis). For comparison of the changes in inputs to inspiratory on- and off-switch with naloxone injection into the same area between cohorts (unpaired data), we used the Mann-Whitney-U test (2 comparisons) or Kruskal-Wallis test (3 comparisons). Hypothesis testing was two-tailed. The critical value for significant differences was adjusted according to the number of comparisons for each protocol according to Bonferroni, i.e., $p < 0.0125$ for 4

comparisons, $p < 0.0167$ for 3 comparisons, and $p < 0.025$ for two comparisons. Results for the different remifentanyl concentrations were analyzed separately without additional correction for multiple comparisons. Inputs to inspiratory on- and off-switch were calculated from the values for inspiratory and expiratory duration as described before (1). Parameters are presented as median (25%–75% range).

Primary outcomes were the changes in respiratory parameters with local microinjection of naloxone at each remifentanyl concentrations, or microinjection of CTAP, naltrindole, and DAMGO, resp.. Secondary outcomes were differences between inputs to inspiratory on- and off-switch depending on order of naloxone reversal and at different remifentanyl concentrations.

Results

In total, 57 animals (34 male/ 23 female) were used for this study. Six animals were used for functional mapping of the caudal medullary raphe with AMPA (2.3.), and four animals were used for the histological confirmation of the injection sites (2.4.). 26 animals were used for the remifentanyl reversal protocols (2.5.–2.7.). One data point (effect of naloxone injection into the PBN/KF, “analgesic” remifentanyl) from six animals in Cohort A was included in our previous publication (1), however, all other data points including the combined naloxone injection into the preBötzinger Complex plus premotor neurons and caudal medullary raphe are new. Data from the animals in Cohort C was used in our previous publication (naloxone injection into the preBötzinger Complex) (1), however, the data presented in the current study including naloxone injection into the preBötzinger Complex plus premotor neurons and caudal medullary raphe have not been reported before. Fourteen animals were used for the opioid antagonist injection protocols (2.8.), and seven animals were used for the DAMGO injection protocol into the caudal medullary raphe (2.9.). Artificial CSF was tested in three animals that were later used for other studies.

3.1.: Opioid effect sites at “analgesic” IV remifentanyl concentrations

To determine the effect of “analgesic” remifentanyl concentrations on the PBN/KF, preBötzinger Complex, and caudal medullary raphe, we microinjected naloxone into these areas in three different orders. The individual values for Cohorts A-C are presented in Table 1, and the level of significance for the naloxone effects are presented in fig.4. In short, remifentanyl infusion depressed respiratory rate by 50%, and sequential naloxone injections *completely reversed* the remifentanyl effect in all cohorts (Cohort A, $p = 0.232$, Cohort B, $p = 0.020$, Cohort C, $p = 0.500$, fig.4B). Additional analysis showed that naloxone injection into the premotor neurons increased respiratory rate by 3 (1–5.75) bpm, compared to naloxone injection into the preBötzinger Complex as defined with functional identification alone ($p < 0.001$, $n = 26$). This effect is already included in the values for preBötzinger Complex injections.

The decrease in respiratory rate was due to an increase in inspiratory (fig.4C) and expiratory duration (fig.4D), which were completely reversed by local naloxone injections. Peak phrenic activity was less affected by “analgesic” remifentanyl concentrations, and naloxone injections into the rhythm generator and caudal medullary raphe increased peak phrenic

activity (fig.4E). Inputs to inspiratory off-switch (derived from inspiratory duration) and on-switch (derived from expiratory duration) were decreased by “analgesic” remifentanyl, and the effect was fully reversed with naloxone microinjections (fig.4F+G).

3.2.: Opioid effect sites at “apneic” IV remifentanyl concentrations

To determine the effect of “apneic” remifentanyl concentrations on the Parabrachial Nucleus/Kölliker-Fuse Complex, preBötzinger Complex, and caudal medullary raphe, we administered an intravenous remifentanyl bolus that caused apnea 1) at baseline, 2) after microinjection of naloxone into the Parabrachial Nucleus/ Kölliker-Fuse Complex and preBötzinger Complex, and 3) after additional naloxone injection into the caudal medullary raphe (Cohort A, n=10). In different animals we administered the “apneic” bolus after naloxone injection in the opposite order, i.e., into the caudal medullary raphe, followed by injections into the preBötzinger Complex and PBN/KF (Cohort B, n=10), or into the preBötzinger Complex, followed by the caudal medullary raphe (Cohort C, n=4). The individual values for Cohorts A-C are presented in Table 2, and the level of significance for the naloxone effects is presented in fig.5. In short, naloxone injection into the target areas *completely prevented* a decrease in respiratory rate from the “apneic” remifentanyl bolus (Cohort A, p=0.695, Cohort B, p=0.074, Cohort C, p=0.500). Additional analysis showed that naloxone injection into the premotor area increased respiratory rate after the “apneic” bolus by 4.5 (2.75–8.5) bpm, compared to naloxone injection into the preBötzinger Complex as defined with functional identification alone (n=13, p<0.001). This effect is already included in the values for preBötzinger Complex injections. After this additional effect was recognized, in subsequent animals, the “apneic” remifentanyl bolus was only injected after naloxone injections into the preBötzinger Complex plus premotor neurons.

Values for inspiratory duration, expiratory duration, and peak phrenic activity were extrapolated from the first breath after apnea (see fig.5A, “control”), or, if no apnea was observed, we averaged parameters for approximately six to eight breaths at the lowest respiratory rate following the remifentanyl bolus (fig.5A, “Naloxone PBN/KF+preBötC” and “Naloxone PBN/KF+preBötC+raphe”). The “apneic” remifentanyl bolus increased inspiratory and, in particular, expiratory duration. This effect was completely prevented by naloxone injections (fig.5, C+D). Peak phrenic activity was less affected (fig.5E). Inputs to inspiratory off-switch (derived from inspiratory duration) and on-switch (derived from expiratory duration) were depressed nearly to the apneic threshold of 1. This effect was completely prevented by naloxone injections (fig.5F+G).

3.3.: Effects of “very high” remifentanyl concentrations on areas outside the Parabrachial Nucleus/Kölliker-Fuse Complex, preBötzinger Complex, and Caudal Medullary Raphe

To determine whether “very high” systemic remifentanyl concentrations affect respiratory rate and tidal volume in other brainstem areas, we injected up to 100 mcg remifentanyl IV after completion of the naloxone microinjection sequence into the PBN/KF, preBötzinger Complex, and caudal medullary raphe (Cohort A+B). Animals without naloxone injection into the PBN/KF (Cohort C) were not included in this analysis. In 19 animals, the “very high” remifentanyl bolus decreased respiratory rate by 10 (5.5–22) bpm (p<0.001) and peak phrenic activity by 32 (20–49)% (p<0.001, fig.6A). Inspiratory duration was increased by

0.1 (0.1–0.4) sec ($p=0.001$), and expiratory duration was increased by 0.35 (0.1–1.4) sec ($p<0.001$). The decrease in respiratory rate from control was 29 (11–54) %, and thus similar in magnitude to the decrease in peak phrenic activity.

Additional analysis determined whether the respiratory rate depression from the “very high” remifentanyl bolus correlated with a lack of reversal of the “analgesic” and “apneic” remifentanyl concentrations, which may have suggested that the naloxone microinjections had insufficiently antagonized the targeted areas. “Very high” remifentanyl resulted in apnea in two animals. In one of these animals, the effect of “analgesic” remifentanyl was completely reversed, but there remained a 38% depression of respiratory rate from the “apneic” bolus, potentially indicating insufficient coverage of the targeted areas. In the other animal, naloxone injections increased respiratory rate above control during “analgesic” and “apneic” remifentanyl concentrations confirming correct injections. Linear regression analysis (fig.6B) showed poor correlation between the respiratory rate depression from “very high” remifentanyl concentrations and any residual respiratory rate depression at “analgesic” ($R^2=0.006$) and “apneic” remifentanyl concentrations ($R^2=0.275$) (fig.6B), suggesting that the effect of the “very high” bolus was due to depression of areas outside the PBN/KF, preBöttinger Complex, and caudal medullary raphe.

We also investigated whether repeated injections of remifentanyl led to attenuation of the respiratory depressive effect. In four animals at the beginning of the study, we injected “apneic” and “very high” remifentanyl boluses after naloxone injection into the PBN/KF and preBöttinger Complex, the premotor neurons, and finally after naloxone injection into the caudal medullary raphe. The final “very high” remifentanyl bolus still caused apnea in one animal, and 5–67% respiratory rate depression in the other animals, while in animals who had received only two “apneic” bolus doses before, the single “very high” remifentanyl bolus resulted in apnea in one animal and a median respiratory rate depression of 20% (31–(–15)%). This suggests that repeated injections did not lead to a systematic attenuation of the remifentanyl-induced respiratory depression during these experiments.

3.4.: Effects of naloxone, CTAP and naltrindole, and aCSF in premotor neurons and the caudal medullary raphe

We injected the non-specific opioid antagonist naloxone into the premotor neurons and the caudal medullary raphe to assess if endogenous opioid receptor activation was present. In four animals, injection of naloxone into the premotor neuron area did not change respiratory rate ($p=0.250$), peak phrenic activity ($p>0.999$), inspiratory ($p=0.875$), or expiratory duration ($p=0.250$).

In seven animals, naloxone injection into the caudal medullary raphe increased respiratory rate from 29 (21–35) to 43 (30–52) bpm ($p=0.016$, fig.7). Peak phrenic activity did not change (100% to 104 (95–145)%, $p=0.297$). Naloxone injection decreased inspiratory duration from 1.0 (0.8–1.1) sec ($p=0.016$) and expiratory duration from 1.1 (0.9–1.7) to 0.8 (0.5–1.2) sec ($p=0.016$). We then sought to confirm that the effect was mediated by opioid receptors and to determine the opioid receptor subtypes. In seven different animals, injection of the mu-receptor antagonist CTAP into the caudal medullary raphe increased respiratory rate from 28 (26–36) to 40 (40–43) bpm ($p=0.016$), and subsequent injection of

the delta-receptor antagonist naltrindole increased rate further to 43 (40–48) bpm ($p=0.016$). Neither CTAP nor naltrindole injection changed peak phrenic activity (100 to 105 (90–116)%, $p=0.688$ and 107 (94–121), $p=0.578$). CTAP injection decreased inspiratory duration from 0.8 (0.8–1.0) to 0.64 (0.6–0.7) sec ($p=0.016$), and naltrindole caused an additional decrease to 0.61 (0.55–0.63) sec ($p=0.016$). CTAP injection decreased expiratory duration from 1.1 (0.9–1.4) to 0.9 (0.7–0.9) sec ($p=0.016$), and naltrindole caused an additional decrease to 0.8 (0.6–0.9) sec ($p=0.016$).

As a control, in three animals we injected aCSF into the caudal medullary raphe before naloxone injection. Artificial CSF did not change respiratory rate ($p>0.999$) or peak phrenic activity ($p>0.999$).

3.5.: Effects of supraclinical concentrations of DAMGO in the Caudal Medullary Raphe

We investigated the effects of supraclinical, saturating concentrations of the mu-opioid receptor agonist DAMGO to determine whether endogenous opioid agonists had maximally activated opioid receptors in the caudal medullary raphe at baseline, i.e., in the absence of exogenous opioid agonists. In seven animals, DAMGO injection into the caudal medullary raphe decreased respiratory rate from 31 (28–35) to 15 (14–21) bpm ($p=0.016$, fig.8). Peak phrenic activity did not change (100 to 80 (66–102)%, $p=0.219$). DAMGO injection increased inspiratory duration from 0.9 (0.8–1.0) to 1.5 (1.1–2.3) sec ($p=0.016$) and increased expiratory duration from 1.1 (0.9–1.2) to 1.8 (1.8–2.8) sec ($p=0.016$).

Additional analysis that compared the DAMGO effects in the caudal medullary raphe with previously published effects in the PBN/KF ($n=6$) (1) showed that the respiratory rate after DAMGO injection into the caudal medullary raphe was higher than after injection into the PBN/KF (15 (14–21) bpm vs. 6 (3–7) bpm, $p=0.001$, Mann-Whitney-U test). Peak phrenic activity after DAMGO injection into the caudal medullary raphe was similar to activity after injection into the PBN/KF (80 (66–102)% vs. 96 (85–108)%, $p=0.366$). Inspiratory duration was less prolonged after DAMGO injection into the caudal medullary raphe compared to the PBN/KF (5.0 (3.9–8.4) sec vs. 1.5 (1.1–2.9) sec, $p=0.001$), as was expiratory duration (1.8 (1.8–2.8) sec vs. 5.4 (4.2–11.3) sec, $p=0.001$).

3.6. Change in inputs to respiratory phase switch with naloxone injection during control conditions, and at “analgesic” and “apneic” remifentanil concentrations

We have previously described that changes in the inputs to inspiratory on- and off-switch allow comparison of naloxone effects on inspiratory and expiratory duration independent of the respiratory rate at the time (1, 8). We now investigated whether the increase in inputs that we observed with naloxone injection into the caudal medullary raphe at “analgesic” and “apneic” remifentanil concentrations was greater than the naloxone reversal of endogenous opioid activity in that area. We also assessed whether the order of naloxone injection, i.e., into the PBN/KF plus preBöttinger Complex before or after naloxone injection into the caudal medullary raphe affected the magnitude of the naloxone effect in the rhythm generator. We calculated the difference in inputs (“delta”) to inspiratory off-switch (fig.9A) and on-switch (fig.9B) from the inspiratory and expiratory duration, resp., before and after naloxone injection into the areas of interest. Statistical comparisons of matching injections

(same location and remifentanyl concentration) from separate cohorts (naloxone injection orders) mostly showed no difference and allowed pooling of the data before further analysis (fig.9C). The deltas for naloxone injection or CTAP plus naltrindole injections into the caudal medullary raphe without intravenous remifentanyl were also of similar magnitude (fig.7) and were pooled before further analysis (n=14). Further analysis provided two insights:

1. Opioid antagonist injections into the caudal medullary raphe caused a similar increase in inputs to inspiratory off-switch (fig.9A, $p=0.311$, Kruskal Wallis) and on-switch (fig.9B, $p=0.262$) without intravenous remifentanyl (n=14) and at “analgesic” (n=26) and “apneic” (n=22) remifentanyl concentrations. We can thus not rule out that the observed “remifentanyl reversal” in the caudal medullary raphe was indeed a reversal of endogenous opioid receptor activation.
2. At “apneic” remifentanyl concentrations, inputs to inspiratory on-switch in the respiratory rhythm generator, i.e., the PBN/KF plus preBötzinger Complex, were increased more after prior naloxone injection into the caudal medullary raphe ($p<0.001$, blue bracket, fig.9B). This suggests that the level of activity of PBN/KF and preBötzinger Complex neurons that promote inspiratory on-switch depends on the excitatory inputs to these areas, and that these inputs are depressed by opioids.

Discussion

This is the first study to show complete reversal of respiratory depression from “analgesic” and “apneic” concentrations of intravenous remifentanyl with sequential naloxone microinjections into the bilateral PBN/KF, preBötzinger Complex, and caudal medullary raphe in vivo. However, “very high” remifentanyl doses continued to cause significant respiratory rate depression despite naloxone antagonism in the above areas, suggesting that such high doses additionally depress respiratory drive outside the injected areas. Naloxone reversal of the PBN/KF and preBötzinger Complex at “apneic” remifentanyl concentrations had a greater effect after prior reversal of the caudal medullary raphe, consistent with our hypothesis that the magnitude of respiratory activity that can be recovered in the respiratory rhythm generator depends on the excitatory drive to these areas. In addition, we demonstrated the presence of *endogenous* mu- and delta-opioid receptor activation in the caudal medullary raphe, which means that the prevailing baseline respiratory rate was already significantly attenuated by endogenous opioids. However, endogenous mu-receptor activation was not maximal because DAMGO microinjection into the caudal medullary raphe caused substantial additional respiratory slowing.

Opioid effects on respiratory drive contribute to opioid-induced respiratory depression

We previously reported that naloxone injection into the PBN/KF and preBötzinger Complex resulted only in incomplete reversal of respiratory depression from “analgesic” and even less from “apneic” remifentanyl concentrations, and we postulated that this was caused by a depression of respiratory drive by opioids to these areas (1). Similarly, Varga et al reported that mu-opioid receptor deletion in the Kölliker-Fuse complex attenuated morphine-induced

respiratory depression, however, higher morphine doses increasingly depressed respiratory rate, suggesting that morphine also decreased the drive to the respiratory rhythm generator (4). The general mechanism was demonstrated in a mouse brainstem slice preparation where excitatory postsynaptic potentials in inspiratory preBötzing Complex neurons that were evoked by photostimulation of contralateral preBötzing Complex neurons were reduced by inhibition of the presynaptic photostimulated, opioid-sensitive neurons with DAMGO (28). Our current study confirms that in addition to reversal of the respiratory rhythm generator, complete reversal of opioid-induced respiratory depression requires antagonizing the opioid effect in the caudal medullary raphe (fig. 4 and 5), an area that contributes drive to multiple areas of the respiratory system including the preBötzing Complex (29), the retrotrapezoid nucleus (30), and phrenic motoneurons (31). The raphe has been described as a relay station for excitatory inputs from the pontine respiratory group to the preBötzing Complex (32). DAMGO injection into the raphe increased inspiratory and expiratory duration (fig.8) although less than DAMGO injection into the PBN/KF (1)(3.5.). On the other hand, reversal of opioid inhibition in the raphe decreased inspiratory and expiratory duration even when the PBN/KF and preBötzing Complex were still inhibited by remifentanyl (fig.4 and 5, F+G, middle), and prior opioid reversal of the raphe increased the respiratory activity that could be recovered with naloxone injection in the respiratory rhythm generator at “apneic” remifentanyl concentrations (fig.9B), all consistent with the caudal medullary raphe as a source of drive to respiratory phase switching neurons. Naloxone injection into the caudal medullary raphe also reduced the respiratory rate depression from “very high” opioid concentrations from ~50% after naloxone reversal solely in the PBN/KF and preBötzing Complex (1) to ~30%, which still was a significant decrease (fig.6). This was likely due to depression of other sources of respiratory drive (see section 3.3.). Only one study investigated opioid effects on the retrotrapezoid nucleus, which is considered the main source of respiratory chemodrive (9, 30, 33), in vivo and reported that chemosensitive neurons were not affected by “apneic” systemic morphine doses (10). Higher doses were not tested. The depression of respiratory drive by high opioid concentrations is of importance as the search for clinically useful, respiratory stimulating drugs continues to focus on the respiratory rhythm generator (34), and a decreased drive to the rhythm generator would limit the efficacy of such targeted drugs.

Endogenous opioid receptor activation in the caudal medullary raphe

Clinical studies in the 1980's and 90's identified elevated levels of endogenous opioids in the cerebrospinal fluid and brain tissue from victims of sudden infant death syndrome (SIDS) and infants with apnea of prematurity (35, 36). Animal studies found that systemic naloxone administration increased respiratory rate and CO₂ sensitivity (37–39), and baseline respiratory rate was higher in mu-opioid receptor knock-out mice (39). However, no study to date was able to identify a specific respiratory related brainstem area that was inhibited by endogenous opioids. To verify that the increase in respiratory rate with naloxone injection into the caudal medullary raphe (fig.7, left) was not due to non-specific actions, e.g., γ -aminobutyric acid (GABA)_A receptor antagonism (40), we repeated the microinjection protocol under baseline conditions with the specific mu-opioid receptor antagonist CTAP followed by the delta-receptor antagonist naltrindole and observed the same effect (fig.7, right). Optogenetic stimulation of pre-opiomelanocortin neurons (POMC) in the sensory

nucleus of the vagus resulted in significant respiratory rate depression that could be antagonized with systemic naloxone in the in situ rat preparation (41). Beta-endorphin is one transmitter released by these neurons, and immunohistochemistry showed synapses in the raphe obscurus (41). Without stimulation systemic naloxone did not increase respiration (41) suggesting that endogenous opioid release may depend on peripheral afferents that were not present in situ.

At this time, we cannot differentiate whether naloxone injection into the caudal medullary raphe during remifentanil administration reversed the exogenous remifentanil effect or antagonized the endogenous ligand (fig.9). “Very high” remifentanil concentrations may depress the caudal medullary raphe beyond the endogenous opioid effect, similarly to local microinjection of supraclinical concentrations of DAMGO (fig.8).

Opioid effects illustrate the distribution of the respiratory network

The impact of opioids in the caudal medullary raphe and other sources of respiratory drive on the respiratory motor output highlights that respiratory rhythm and pattern are determined by the activity of a wide neuronal network that is integrated by the PBN/KF and preBötzinger Complex. In the in situ perfused brainstem preparation, local field potentials were distributed throughout the ponto-medullary respiratory column with high synchronization during respiratory phase transitions in the preBötzinger Complex, PBN/KF, and dorsal respiratory group (42). Cross-correlation analysis in vivo showed excitatory projections from chemoreceptive neurons in the retrotrapezoid nucleus to the preBötzinger Complex and ventral respiratory group (43), and peripheral chemoreceptor input led to disinhibition of inspiratory neurons in the same areas (44). In addition, extensive connections exist between brainstem respiratory nuclei and higher brain regions. Retrograde tracer studies demonstrated direct projections from cortex and hypothalamus to the Periaqueductal Gray, Kölliker-Fuse Nucleus, preBötzinger Complex, and caudal medullary raphe (45), and additional projections from the Periaqueductal Gray to these areas (46). Electrical or chemical stimulation of subareas of the Periaqueductal Gray elicited variable changes in respiratory pattern (review by (47)). These connections likely provide the neuronal basis for the effects of volition, emotion, and awake state on respiratory rhythm and pattern. Projections from the medulla and in particular from the Kölliker-Fuse Nucleus to the Periaqueductal Gray suggest a feedback loop (46). Many of these forebrain areas are affected by local or systemic opioid application (see review in (8)).

Methodological considerations

Localization of the caudal medullary raphe: Functional mapping of the midline raphe showed excitatory responses to AMPA injection between obex and approximately halfway between the preBötzinger Complex level and the caudal end of the facial nucleus (fig.1). In the anesthetized cat, electrical or glutamate stimulation in a comparable area increased phrenic activity; the area was considered raphe obscurus (48, 49), while stimulation of the raphe pallidus could increase or decrease phrenic output (49). In anesthetized rats, electrical stimulation of the raphe obscurus caused bradypnea (50) or a mix of tachypnea and bradypnea (51), while stimulation of the raphe pallidus caused tachypnea (50, 51). Another rat study observed a mix of respiratory rate increase and

decrease with glutamate agonist injections into the midline raphe in different animals between -11.6 to -12.0 mm caudal from bregma (17), i.e., in the area between the facial nucleus and preBötzing Complex, which matches our experience in rabbits. Mu-opioid receptors were histologically shown in the raphe pallidus (52), but axonal projections of beta-endorphin-releasing POMC neurons were also identified in the raphe obscurus and paramedian reticular nucleus (41). Since the borders between these areas are not clearly demarcated (see the excellent discussion in (53)), for this first study we performed relatively large naloxone injections into both, the raphe pallidus and raphe obscurus and refer to the entire area as the caudal medullary raphe. The area is likely larger than the area reached with CTAP injections into the “caudal medullary raphe” by Zhang et al., which were performed at a single rostro-caudal coordinate at the level of the preBötzing Complex (11). The additional increase in respiratory rate we observed with each injection caudal to, at the level of, and rostral to the preBötzing Complex level (fig.7) suggested endogenous opioid receptor activation over the entire extent of injections. We do not expect a confounding effect from diffusion of these injections (2×350 nl) to the ventral respiratory group because 700nl naloxone injections into the preBötzing Complex (1) and premotor neuron area (section 3.4.) did not change respiratory rate, suggesting a sufficient distance between these areas.

Rostro-caudal dimensions of the preBötzing Complex: The preBötzing Complex is considered to be a small, circumscribed area characterized by neurokinin receptor-1 and somatostatin positive neurons (5, 54). Injection volumes were traditionally small to avoid effects in adjacent neuron groups (55, 56), however, Baertsch et al. demonstrated that the range of neurons whose stimulation prompted an inspiratory burst extended from 1mm caudal to 1.5mm rostral of the “preBötzing Complex center” in horizontal mouse slices and depended on the balance between excitatory and inhibitory drive to the preparation (57). We chose an injection volume of 700nl for preBötzing Complex injections because DAMGO (26) and glutamate antagonist (14) injections into the same area using this volume were sufficient to cause apnea. We have previously reported that additional naloxone injection caudal to the preBötzing Complex led to a small increase in respiratory rate reversal (1 (0–3) bpm) during “analgesic” remifentanyl infusion (1). In the current study, we routinely injected naloxone into the area of the premotor neurons, which increased the remifentanyl reversal. Interestingly, apnea from the “apneic” bolus was reliably prevented in all five animals after naloxone injection into the preBötzing Complex plus premotor neurons (fig.5B, right) while in a previous study, injection into the preBötzing Complex alone had prevented apnea only in 2/9 animals (1). This suggests that the area that contributes to inspiratory on-switch and is depressed by systemic opioids extends beyond the estimated spheric diameter of 1–1.2mm around the electrode tip that is reached by a single naloxone injection in our model (14).

Conclusion

Opioid reversal in the Parabrachial Nucleus/Kölliker-Fuse Complex, preBötzing Complex, and caudal medullary raphe completely reversed respiratory depression from “analgesic” and “apneic” remifentanyl concentrations. “Very high” remifentanyl doses still depressed respiratory rate and peak phrenic activity suggesting depression of respiratory drive at very

high opioid concentrations. We also found substantial endogenous opioid receptor activation in the caudal medullary raphe that was mediated by mu- and delta-opioid receptors. Taken together, our results point to the importance of the depression of respiratory drive by high opioid doses for opioid-induced respiratory depression.

Acknowledgements:

The authors thank Andrew Williams (Engineering Technician, Medical College of Wisconsin, Milwaukee, WI) for his outstanding support with the experimental setup and Dr. Pippa Simpson, Director Division of Quantitative Health Sciences, for her advice with the statistical analysis.

Funding statement:

This work was supported by the NIH (R01-GM112960, Dr. Stucke).

References

1. Palkovic B, Callison J, Marchenko V, Stuth E, Zuperku E, Stucke A. Dose-dependent respiratory depression by remifentanyl in the Parabrachial Nucleus/ Kölliker-Fuse Complex and preBötzing Complex in in vivo rabbits. *Anesthesiology*. 2021;ePub before print.
2. Levitt E, Abdala AP, Paton JFR, Bissonnette JM, Williams JT. Mu-opioid receptor activation hyperpolarizes respiratory-controlling Kölliker-Fuse neurons and suppresses post-inspiratory drive. *J Physiol*. 2015;593:4453–69. [PubMed: 26175072]
3. Saunders S, Levitt E. Kölliker-Fuse/Parabrachial complex mu opioid receptors contribute to fentanyl-induced apnea and respiratory rate depression. *Resp Physiol Neurobiol*. 2020;275:103388.
4. Varga GA, Reid BT, Kieffer BL, Levitt ES. Differential impact of two critical respiratory centres in opioid-induced respiratory depression in awake mice. *J Physiol*. 2020;598:189–205. [PubMed: 31589332]
5. Bachmutsky I, Wei X, Kish E, Yackle K. Opioids depress breathing through two small brainstem sites. *eLife*. 2020;9:e52694. [PubMed: 32073401]
6. Miller J, Zuperku E, Stuth E, Banerjee A, Hopp F, Stucke A. A Subregion of the Parabrachial Nucleus Partially Mediates Respiratory Rate Depression from Intravenous Remifentanyl in Young and Adult Rabbits. *Anesthesiology*. 2017;127(3):502–14. [PubMed: 28590302]
7. Prkic I, Mustapic S, Radocaj T, Stucke AG, Stuth EA, Hopp FA, et al. Pontine mu-opioid receptors mediate bradypnea caused by intravenous remifentanyl infusions at clinically relevant concentrations in dogs. *J Neurophysiol*. 2012;108(9):2430–41. [PubMed: 22875901]
8. Palkovic B, Marchenko V, Zuperku E, Stuth E, Stucke A. Multi-level regulation of opioid-induced respiratory depression. *Physiology*. 2020;35:391–404. [PubMed: 33052772]
9. Guyenet P, Stornetta R, Souza G, Abbott A, Shi Y, Bayliss D. The retrotrapezoid nucleus: central chemoreceptor and regulator of breathing automaticity. *Trends in Neurosciences*. 2019;42:807–24.
10. Mulkey DK, Stornetta RL, Weston MC, Simmons JR, Parker A, Bayliss DA, et al. Respiratory control by ventral surface chemoreceptor neurons in rats. *Nat Neurosci*. 2004;7(12):1360–9. [PubMed: 15558061]
11. Zhang Z, Xu F, Zhang C, Liang X. Activation of opioid mu receptors in caudal medullary raphe region inhibits the ventilatory response to hypercapnia in anesthetized rats. *Anesthesiology*. 2007;107(2):288–97. [PubMed: 17667574]
12. Phillips RS, Cleary DR, Nalwalk JW, Arttamangkul S, Hough LB, Heinricher MM. Pain-facilitating medullary neurons contribute to opioid-induced respiratory depression. *J Neurophysiol*. 2012;108(9):2393–404. [PubMed: 22956800]
13. Dogas Z, Krolo M, Stuth EA, Tonkovic-Capin M, Hopp FA, McCrimmon DR, et al. Differential effects of GABA_A receptor antagonists in the control of respiratory neuronal discharge patterns. *J Neurophysiol*. 1998;80:2368–77. [PubMed: 9819249]
14. Cook-Snyder D, Miller JR, Navarrete-Opazo AA, Callison JJ, Peterson RC, Hopp FA, Stuth EA, Zuperku EJ, Stucke AG. The contribution of endogenous glutamatergic input in the ventral

- respiratory column to respiratory rhythm. *Respir Physiol Neurobiol.* 2019;260:37–52. [PubMed: 30502519]
15. Eldridge FL. Expiratory effects of brief carotid sinus nerve and carotid body stimulations. *Respir Physiol.* 1976;26:395–410.
 16. Navarrete-Opazo A, Cook-Snyder D, Miller J, Callison J, McCarthy N, Palkovic B, et al. Endogenous glutamatergic inputs to the Parabrachial Nucleus/ Kölliker-Fuse Complex determine respiratory rate. *Respir Physiol Neurobiol.* 2020;277:103401.
 17. Verner T, Goodchild A, Pilowski P. A mapping study of cardiorespiratory responses to chemical stimulation of the midline medulla oblongata in ventilated and freely behaving rats. *Am J Physiol Regul Integr Comp Physiol.* 2004;287:R411–21. [PubMed: 15031133]
 18. Dias M, Nucci T, Branco L, Gargaglioni L. Opioid mu-receptors in the rostral medullary raphe modulate hypoxia-induced hyperpnea in unanesthetized rats. *Acta Physiol.* 2012;204:435–42.
 19. Meessen H, Olszewski J. *Cytoarchitectonischer Atlas des Rautenhirns des Kaninchens.* Basel: Karger; 1949.
 20. Felten D, Cummings J. The raphe nuclei of the rabbit brainstem. *J Comp Neur.* 1979;187:199–244. [PubMed: 114552]
 21. Ma D, Chakrabarti MK, Whitwam JG. Effects of propofol and remifentanyl on phrenic nerve activity and nociceptive cardiovascular responses in rabbits. *Anesthesiology.* 1999;91(5):1470–80. [PubMed: 10551600]
 22. Michelsen LG, Salmenpera M, Hug CC Jr., Szlam F, VanderMeer D. Anesthetic potency of remifentanyl in dogs. *Anesthesiology.* 1996;84(4):865–72. [PubMed: 8638841]
 23. Flecknell P, Mitchell M. Midazolam and fentanyl-flanision: assessment of anaesthetic effects in laboratory rodents and rabbits. *Laboratory Animals.* 1984;18:143–6. [PubMed: 6748593]
 24. Hayashida M, Fukunaga A, Hanaoka K. Detection of acute tolerance to the analgesic and nonanalgesic effects of remifentanyl infusion in a rabbit model. *Anesthesia Analgesia.* 2003;97:1347–52. [PubMed: 14570650]
 25. Montandon G, Qin W, Liu H, Ren J, Greer JJ, Horner RL. PreBotzinger complex neurokinin-1 receptor-expressing neurons mediate opioid-induced respiratory depression. *J Neurosci.* 2011;31(4):1292–301. [PubMed: 21273414]
 26. Stucke AG, Miller JR, Prkic I, Zuperku EJ, Hopp FA, Stuth EA. Opioid-induced Respiratory Depression Is Only Partially Mediated by the preBotzinger Complex in Young and Adult Rabbits In Vivo. *Anesthesiology.* 2015;122(6):1288–98. [PubMed: 25751234]
 27. Mustapic S, Radocaj T, Sanchez A, Dogas Z, Stucke AG, Hopp FA, et al. Clinically relevant infusion rates of mu-opioid agonist remifentanyl cause bradypnea in decerebrate dogs but not via direct effects in the pre-Botzinger complex region. *J Neurophysiol.* 2010;103(1):409–18. [PubMed: 19906886]
 28. Baertsch N, Bush N, Burgraff N, Ramirez J. Dual mechanisms of opioid-induced respiratory depression in the inspiratory rhythm-generating network. *eLife.* 2021;10:e67523. [PubMed: 34402425]
 29. Ptak K, Yamanishi T, Aungst J, Milescu LS, Zhang R, Richerson GB, et al. Raphe neurons stimulate respiratory circuit activity by multiple mechanisms via endogenously released serotonin and substance P. *J Neurosci.* 2009;29(12):3720–37. [PubMed: 19321769]
 30. Wu Y, Proch K, Teran F, Lechtenberg R, Kothari H, Richerson G. Chemosensitivity of Phox2b-expressing retrotrapezoid neurons is mediated in part by input from 5-HT neurons. *J Physiol.* 2019;597:2741–66. [PubMed: 30866045]
 31. Holtman JR Jr., Norman WP, Gillis RA. Projections from the raphe nuclei to the phrenic motor nucleus in the cat. *Neurosci Lett.* 1984;44(1):105–11. [PubMed: 6717845]
 32. Nuding SC, Segers LS, Baekey DM, Dick TE, Solomon IC, Shannon R, et al. Pontine-ventral respiratory column interactions through raphe circuits detected using multi-array spike train recordings. *J Neurophysiol.* 2009;101(6):2943–60. [PubMed: 19297509]
 33. Silva J, Lucena EV, Silva TM, Damasceno RS, Takakura AC, Moreira TS. Inhibition of the pontine Kölliker-Fuse nucleus reduces genioglossal activity elicited by stimulation of the retrotrapezoid chemoreceptor neurons. *Neuroscience.* 2016;328:9–21. [PubMed: 27126558]

34. Dahan A, van der Schrier R, Smith T, Aarts L, van Velzen M, Niesters M. Averting opioid-induced respiratory depression without affecting anesthesia. *Anesthesiology*. 2018;128:1027–37. [PubMed: 29553984]
35. Coquerel ABM, Tayot J, Pfaff F, Matray F, Proust B. . Beta-endorphin and neurotensin in brainstem and cerebrospinal fluid in the sudden infant death syndrome. *Neurochem Int*. 1992;20(97–102).
36. Hollander N Beta-endorphin in the brainstem, pituitary, and spinal fluid of infants at autopsy: relation to sudden infant death syndrome. *Forensic Sci Int*. 1988;38:67–74. [PubMed: 2973425]
37. Lawson EE, Waldrop TG, Eldridge FL. Naloxone enhances respiratory output in cats. *J Appl Physiol*. 1979;47(5):1105–11. [PubMed: 511712]
38. Beubler E Naloxone increases carbon dioxide stimulated respiration in the rabbit. *Naunyn Schmiedebergs Arch Pharmacol*. 1980;311(2):199–203. [PubMed: 6770274]
39. Dahan A, Sarton E, Teppema L, Cees O, Niewenhuijs D, Matthes HWD, et al. Anesthetic potency and influence of morphine and sevoflurane on respiration in μ -opioid receptor knockout mice. *Anesthesiology*. 2001;94(5):824–32. [PubMed: 11388534]
40. Gruol D, Barker J, Smith T. Naloxone antagonism of GABA-evoked membrane polarizations in cultured mouse spinal cord neurons. *Brain Research*. 1980;198:323–32. [PubMed: 6250670]
41. Cerritelli S, Hirschberg A, Hill R, Balthasar N, Pickering A. Activation of brainstem pro-opiomelanocortin neurons produces opioidergic analgesia, bradycardia and bradypnoea. *PLoS ONE*. 2016;11(4):e0153187. [PubMed: 27077912]
42. Dhingra R, Dick T, Furuya W, Galan R, Dutschmann M. Volumetric mapping of the functional neuroanatomy of the respiratory network in the perfused brainstem preparation of rats. *J Physiol*. 2020;598.11:2061–79. [PubMed: 32100293]
43. Ott MM, Nuding SC, Segers LS, O'Connor R, Morris KF, Lindsey BG. Central chemoreceptor modulation of breathing via multipath tuning in medullary ventrolateral respiratory column circuits. *J Neurophysiol*. 2012;107(2):603–17. [PubMed: 21994272]
44. Segers LS, Nuding SC, Ott MM, Dean JB, Bolser DC, O'Connor R, et al. Peripheral chemoreceptors tune inspiratory drive via tonic expiratory neuron hubs in the medullary ventral respiratory column network. *J Neurophysiol*. 2015;113(1):352–68. [PubMed: 25343784]
45. Trevizan-Bau P, Dhingra R, Furuya W, Stanic D, Mazzone S, Dutschmann M. Forebrain projection neurons target functionally diverse respiratory control areas in the midbrain, pons, and medulla oblongata. *J Comp Neur*. 2021;529:2243–64. [PubMed: 33340092]
46. Trevizan-Bau P, Furuya W, Mazzone S, Stanic D, Dhingra R, Dutschmann M. Reciprocal connectivity of the periaqueductal gray with the ponto-medullary respiratory network in rat. *Brain Research*. 2021;1757:147255. [PubMed: 33515533]
47. Subramanian H, Holstege G. The midbrain periaqueductal gray changes the eupneic respiratory rhythm into a breathing pattern necessary for survival of the individual and of the species. *Progress in Brain Research*. 2014;212:351–84. [PubMed: 25194206]
48. Holtman JR Jr., Anastasi NC, Norman WP, Dretchen KL. Effect of electrical and chemical stimulation of the raphe obscurus on phrenic nerve activity in the cat. *Brain Res*. 1986;362(2):214–20. [PubMed: 2867815]
49. Holtman JR Jr., Dick TE, Berger AJ. Involvement of serotonin in the excitation of phrenic motoneurons evoked by stimulation of the raphe obscurus. *J Neurosci*. 1986;6(4):1185–93. [PubMed: 3701414]
50. Besnard S, Denise P, Cappelin B, Dutschmann M, Gestreau C. Stimulation of the rat medullary raphe nuclei induces differential responses in respiratory muscle activity. *Respiratory Physiology & Neurobiology*. 2009;165(2–3):208–14. [PubMed: 19135182]
51. Cao Y, Fujito Y, Matsuyama K, Aoki M. Effects of electrical stimulation of the medullary raphe nuclei on respiratory movement in rats. *J Comp Physiol A Neuroethol Sens Neural Behav Physiol*. 2006;192(5):497–505. [PubMed: 16404604]
52. Ding YQ, Kaneko T, Nomura S, Mizuno N. Immunohistochemical localization of μ -opioid receptors in the central nervous system of the rat. *J Comp Neurol*. 1996;367(3):375–402. [PubMed: 8698899]

53. Blessing W, Nalivaiko E. Regional blood flow and nociceptive stimuli in rabbits: patterning by medullary raphe, not ventrolateral medulla. *J Physiol.* 2000;524:279–92. [PubMed: 10747198]
54. Gray P, Hayes J, Ling G, Llona I, Tupal S, Picardo M, et al. Developmental origin of preBötzinger Complex respiratory neurons. *J Neuroscience.* 2010;30:14883–95.
55. Mutolo D, Bongianni F, Nardone F, Pantaleo T. Respiratory responses evoked by blockades of ionotropic glutamate receptors within the Botzinger complex and the pre-Botzinger complex of the rabbit. *Eur J Neurosci.* 2005;21(1):122–34. [PubMed: 15654849]
56. Cinelli E, Bongianni F, Pantaleo T, Mutolo D. Activation of mu-opioid receptors differentially affects the preBötzinger Complex and neighbouring regions of the respiratory network in the adult rabbit. *Resp Physiol Neurobiol.* 2020;280:103482.
57. Baertsch N, Severs L, Anderson T, Ramirez J. A spatially dynamic network underlies the generation of inspiratory behaviors. *PNAS.* 2019;116:7493–502. [PubMed: 30918122]

Highlights:

- Increasing opioid doses differentially affect respiratory-related brainstem areas
- Opioid effects on the rhythm generator profoundly impact respiratory phase timing
- Opioid-induced depression of respiratory drive reduces activity in the rhythm generator
- Exogenous opioids reduce activity of the caudal medullary raphe
- The caudal medullary raphe is partly depressed by endogenous opioids

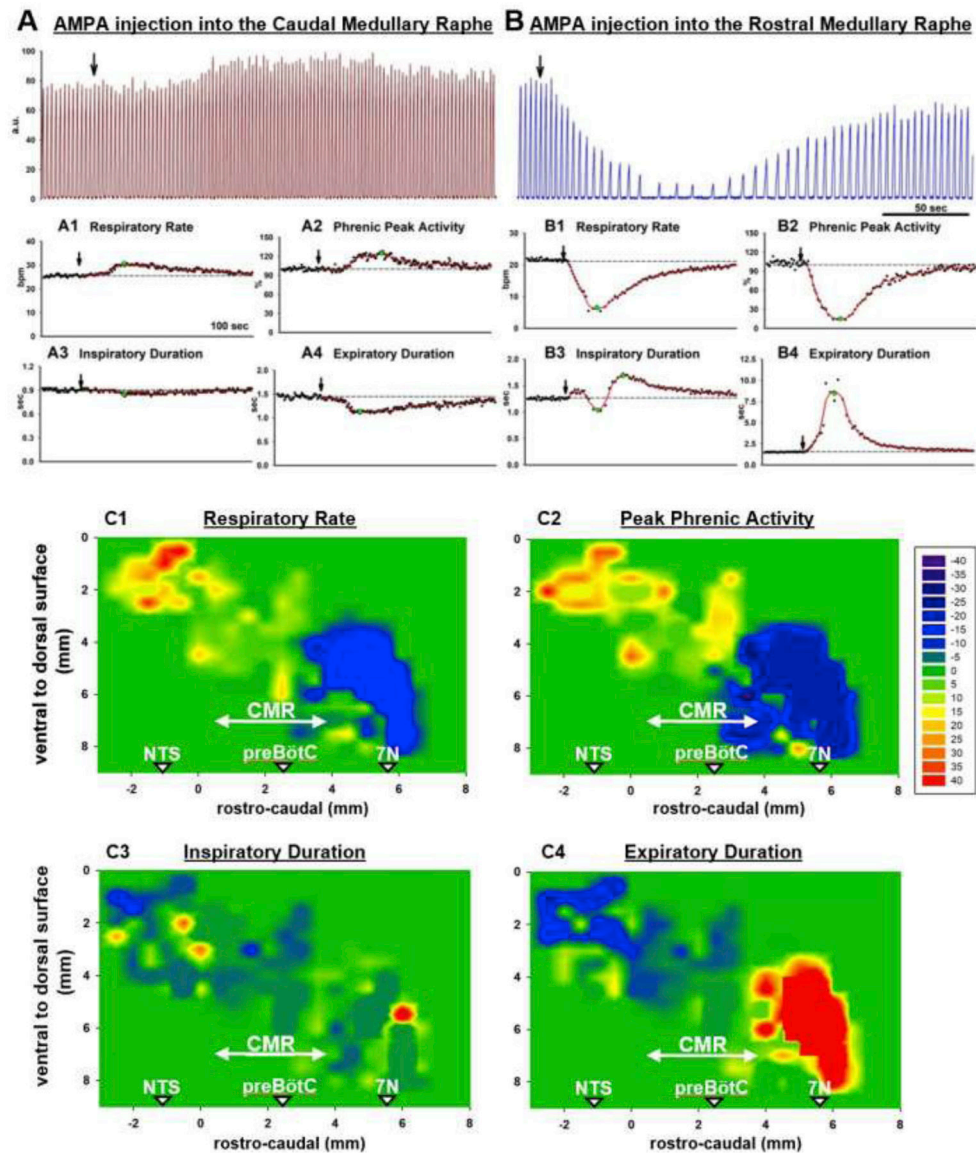


Figure 1,
 A+B: Examples of the Phrenic Neurogram (a.u., arbitrary units) with AMPA injection into (A) the Caudal Medullary Raphe, the area comprised of the raphe pallidus and obscurus, and (B) the Rostral Medullary Raphe, which is located towards the caudal end of the facial nucleus. AMPA injection (black arrow) into the Caudal Medullary Raphe increased respiratory rate (A1, breaths/min, bpm) and peak phrenic activity (A2, %, normalized to control). Inspiratory duration was not changed (A3), but expiratory duration was decreased (A4). AMPA injection into the Rostral Medullary Raphe severely decreased respiratory rate (B1) and peak phrenic activity (B2), consistent with activation of the GABAergic neurons of the Raphe Magnus. Inspiratory duration was often variable (B3) while expiratory duration was increased (B4). C: Contour plots for the changes in respiratory parameters with AMPA injection, based on six animals. AMPA (70nl) was injected in the midline with stepsize 0.47mm rostral-caudal (0.5mm, corrected for an angle of 20° between brainstem and

head holder) and 0.5mm ventro-dorsal, starting at the ventral limit of neuronal discharge. Values for percent change from baseline were aligned relative to the functionally identified preBötzinger Complex (preBötC) and the average plotted for an assumed preBötC location at 2.5mm rostral to obex (obex=0). An increase in respiratory rate was observed between 2mm caudal to and 1.5mm rostral to the preBötC. This area was considered the caudal medullary raphe (CMR, arrow) for study purposes. The area was rostral to the nucleus of the solitary tract (NTS) where AMPA injection caused a prompt increase in respiratory rate and peak phrenic activity and ~1.5mm caudal to the caudal end of the facial nucleus (7N). Scale: 40% (red) to -40% (purple) from baseline, green: no change.

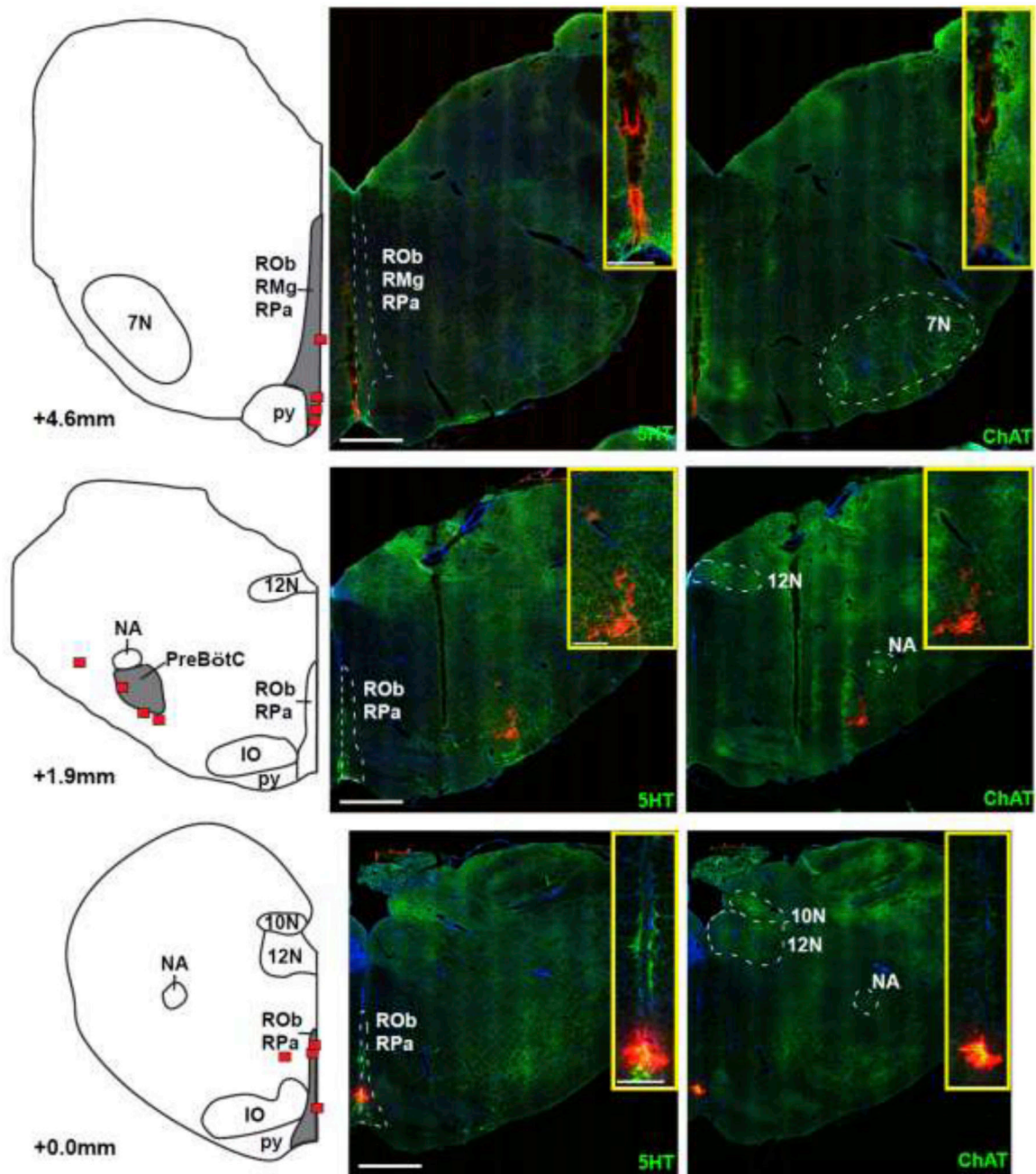


Figure 2: Locations of the caudal end of the Caudal Medullary Raphe (lower), the preBötzinger Complex (preBötC, middle), and the caudal end of the facial nucleus (7N, upper) as identified by injection of fluorescent latex microspheres in four rabbits. The left panel shows diagrammatic hemisections of the brainstem at each rostro-caudal level with the individual injection sites superimposed in red squares. The right panels show the corresponding hemisections from one animal with immunoreactivity for 5-hydroxytryptophan (5HT), representing serotonergic neurons and choline acetyltransferase (ChAT), representing cholinergic (motor) neurons, superimposed over nuclear staining with DAPI. Red

microspheres mark the injection sites. Injection protocols did not differentiate between raphe pallidus (RPa) and raphe obscurus (ROb). IO: inferior olive; py: pyramidal tract; 12N: nucleus hypoglossus; 10N: nucleus nervi vagi; NA: nucleus ambiguus; RMg: raphe magnus. Bar = 1mm. The inserts show zoomed images of the injection sites. Bar = 0.25mm.

Author Manuscript

Author Manuscript

Author Manuscript

Author Manuscript

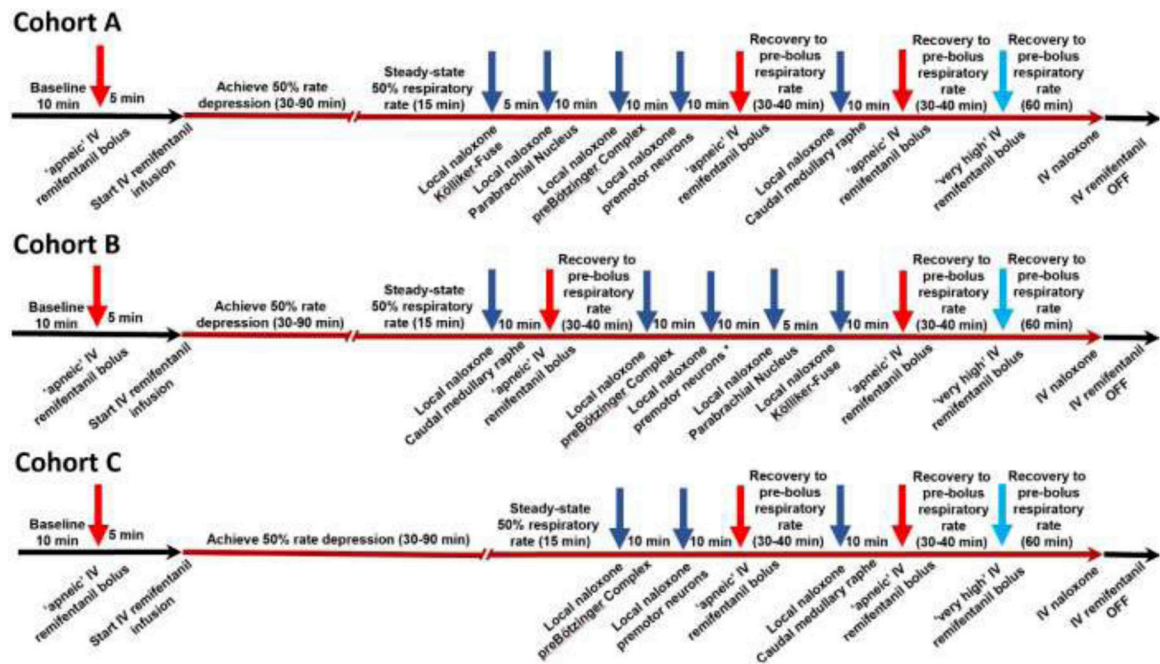
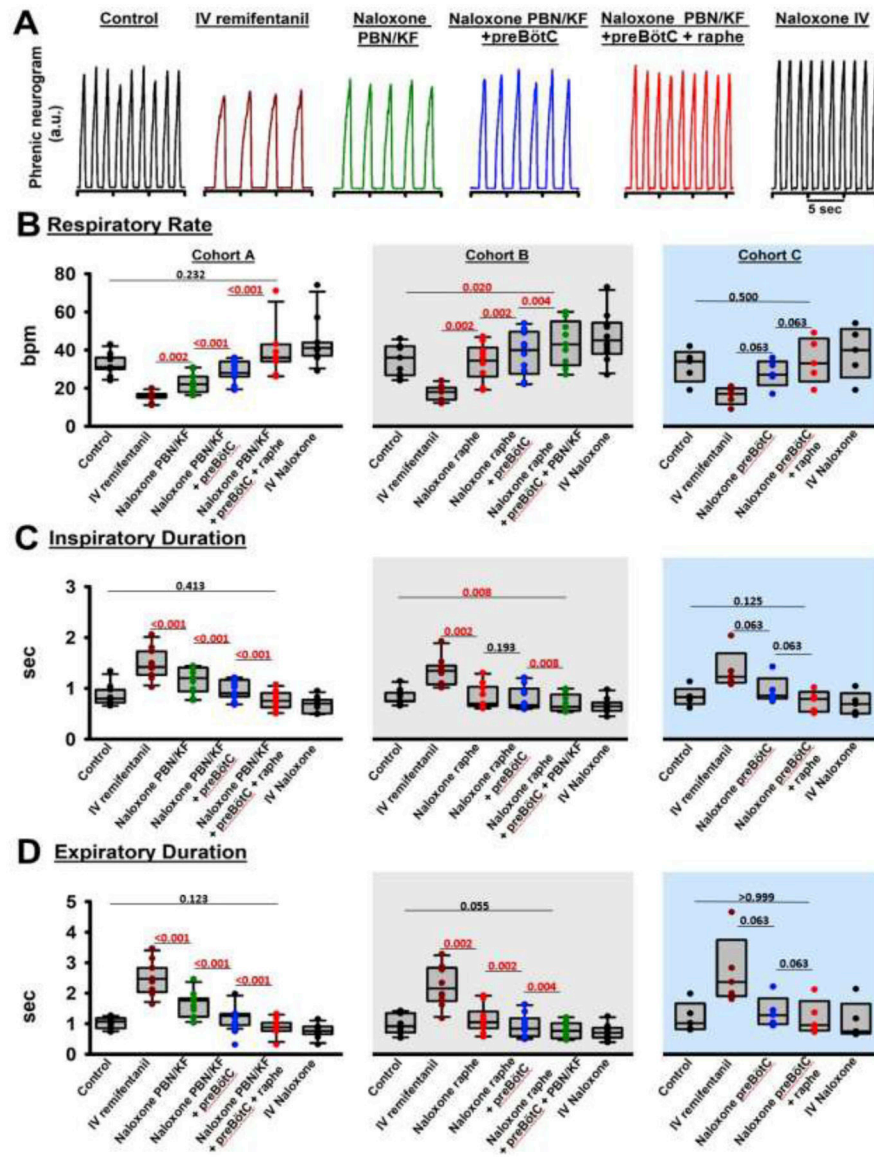


Figure 3:

Injection sequence for intravenous remifentanyl and local naloxone microinjections. The initial intravenous remifentanyl bolus (red arrow) was chosen to cause apnea for more than 60s. Once respiratory activity returned, the remifentanyl infusion was started (red line) until steady-state respiratory rate depression of 50%. This dose-rate was continued unchanged throughout the entire injection sequence. For Cohort A (n=11), naloxone (dark blue arrows) was microinjected into the bilateral Kölliker-Fuse Nucleus, Parabrachial Nucleus, preBötzinger Complex (including premotor neurons), and Caudal Medullary Raphe. Apneic remifentanyl boluses (red arrows) were given after naloxone injections into the pons and preBötzinger Complex, and after subsequent naloxone injection into the raphe. After each “apneic” remifentanyl bolus, we awaited complete recovery of the respiratory rate to prebolus levels before continuing the protocol. The “very high” remifentanyl bolus was administered shortly after the last “apneic” bolus to maximize effect (light blue arrow). In Cohort B (n=10), naloxone was microinjected in the reverse order. In Cohort C, naloxone was microinjected only into the preBötzinger Complex including the premotor neurons and caudal medullary raphe. This protocol was truncated after five animals.



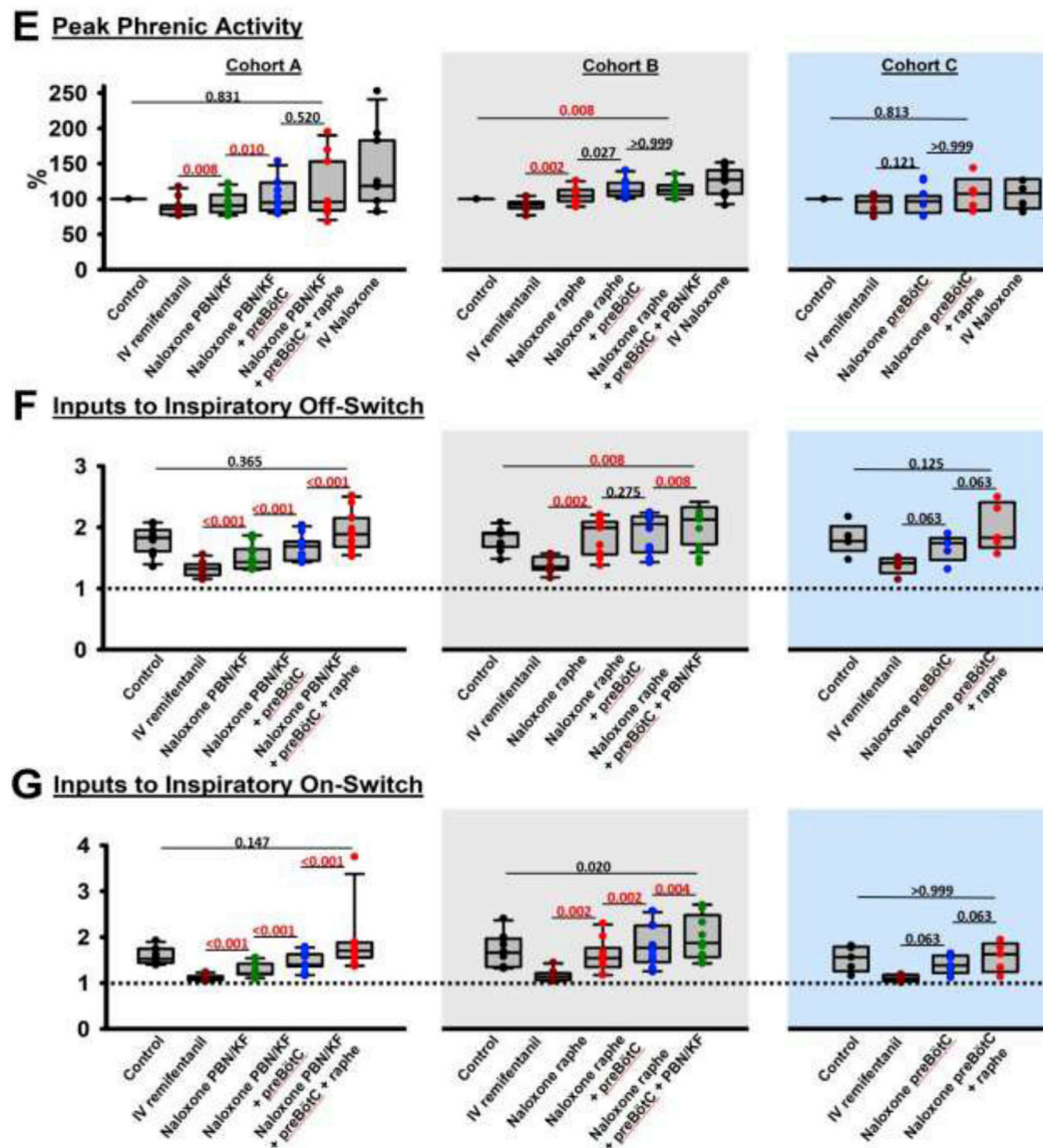


Figure 4: Analgesic remifentanyl concentrations. Bilateral naloxone injection into the Parabrachial Nucleus/Kölliker-Fuse Complex (PBN/KF), the preBötzing Complex including the premotor neurons (preBötC), and the Caudal Medullary Raphe (raphe) completely reversed the respiratory rate depression from intravenous remifentanyl at analgesic concentrations (50% respiratory rate depression). A: Phrenic neurogram tracings during control conditions and sequential drug injections in one rabbit. (B-E) Pooled data for measured respiratory parameters and (F,G) values for the inputs to inspiratory off-switch and on-switch, derived from inspiratory and expiratory duration. Data are presented separately for Cohort A (left panels in white, n=11), Cohort B (center panels in grey, n=10), and Cohort C (right panels in blue, n=5). Bars indicate that the difference between values from two subsequent injections or control was tested against no change (Wilcoxon signed rank test). The levels of significance below the critical $P=0.0125$ are highlighted in red. The dotted line indicates the

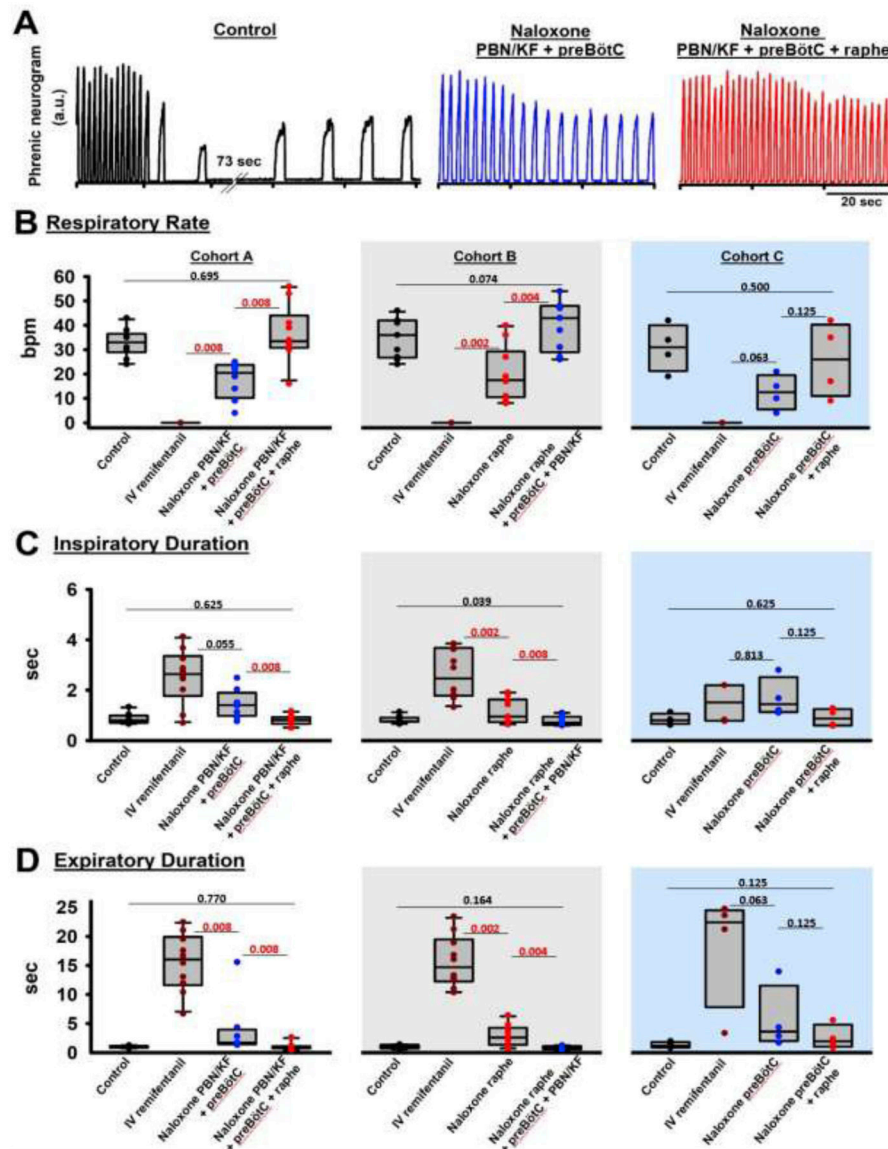
threshold value, set at 1 in our model, which the sum of inputs must exceed to result in phase switch (see Appendix 1 in (1)).

Author Manuscript

Author Manuscript

Author Manuscript

Author Manuscript



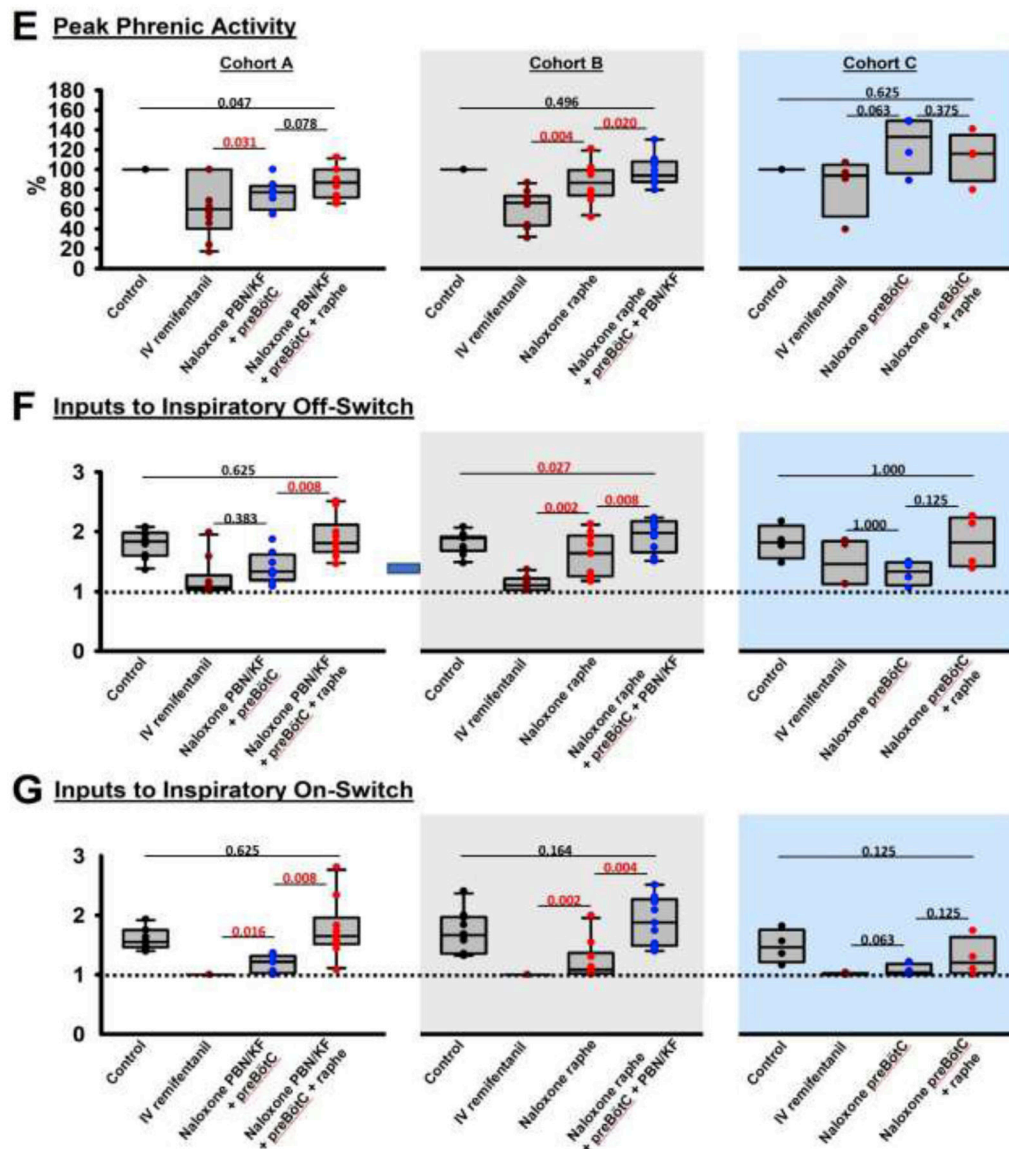


Figure 5: “Apneic” remifentanyl concentrations. Bilateral naloxone injection into the Parabrachial Nucleus/Kölliker-Fuse Complex (PBN/KF), the preBötzinger Complex including the premotor neurons (preBötC), and the Caudal Medullary Raphe (raphe) completely prevented the respiratory rate depression from an intravenous remifentanyl bolus that caused apnea >60sec under control conditions. A: Phrenic neurogram tracings from the same rabbit shown in figure 4 shows that sequential naloxone injections increasingly reduced respiratory rate depression from the “apneic” bolus. (B-E) Pooled data for measured respiratory parameters and (F,G) values for the inputs to inspiratory off-switch and on-switch, derived from inspiratory and expiratory duration. Data are presented separately for Cohort A (left panels in white, n=10), Cohort B (center panels in grey, n=10), and Cohort C (right panels in blue, n=4). Bars indicate that the difference between values from two subsequent injections or control was tested against no change (Wilcoxon signed rank test). The levels of significance

below the critical $P=0.0167$ are highlighted in red. The dotted line indicates the threshold value, set at 1 in our model, which the sum of inputs must exceed to result in phase switch (see Appendix 1 in (1)).

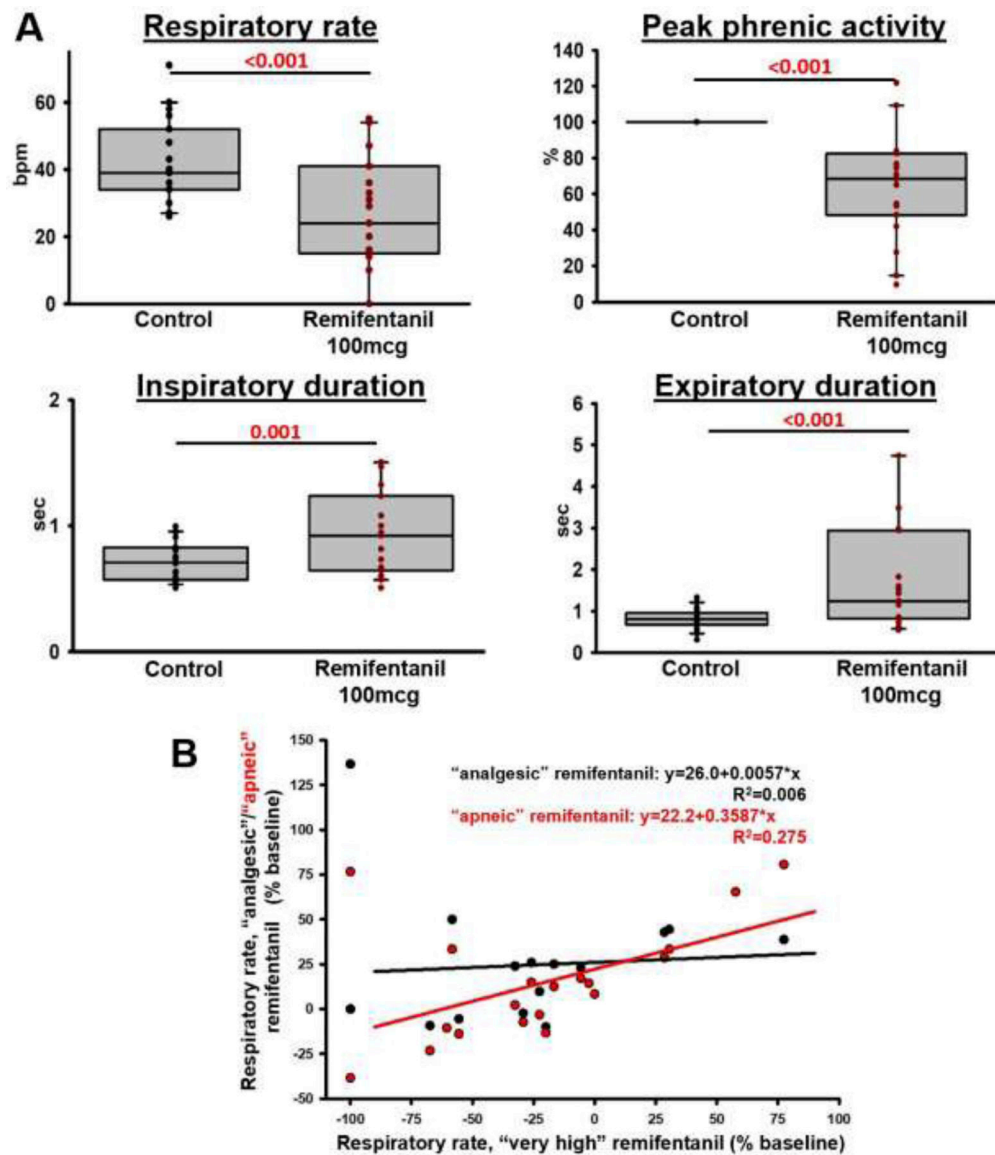


Figure 6: "Very high" remifentanil concentrations. A: After naloxone injection into the bilateral Parabrachial Nucleus/Kölliker-Fuse Complex, preBötzing Complex including premotor neurons, and the Caudal Medullary Raphe, remifentanil was injected intravenously until apnea or to a maximal dose of 100 mcg. In 19 animals, the bolus caused a significant change in all parameters (Wilcoxon signed rank test, critical $P < 0.05$). B: To determine whether the effect of "very high" remifentanil was due to insufficient antagonism of above brainstem regions, we plotted the difference between respiratory rate after the "very high" remifentanil bolus and baseline respiratory rate versus the difference from baseline for "analgesic" (black) and "apneic" (red) remifentanil concentrations at the end of the naloxone injection sequence. Values < 0 indicate a decreased respiratory rate compared to baseline, i.e., -100% indicates apnea. Values > 0 indicate an increased respiratory rate compared to baseline, which was not infrequently seen after naloxone injection into the raphe. Linear

regression analysis showed little correlation between the “very high” remifentanil effect and level of reversal of “analgesic” and “apneic” remifentanil concentrations, suggesting that the naloxone injections correctly antagonized the study areas and that “very high” remifentanil concentrations depressed other areas of respiratory drive.

Author Manuscript

Author Manuscript

Author Manuscript

Author Manuscript

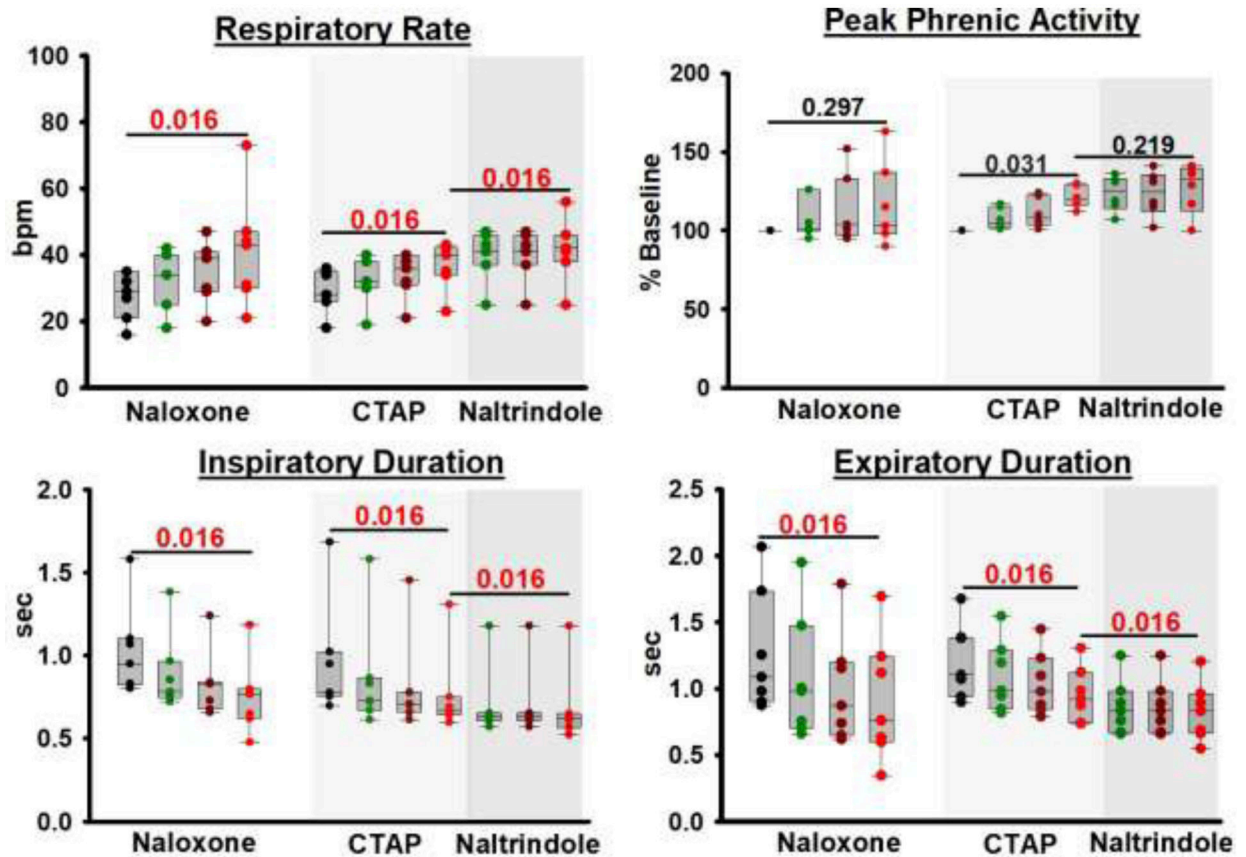


Figure 7:

Opioid antagonist injections into the Caudal Medullary Raphe without systemic remifentanyl. Naloxone injection ($n=7$, left) and, in a separate set of animals, sequential injections of CTAP ($n=7$, middle, light grey) and subsequently naltrindole (right, dark grey) significantly increased respiratory rate. To illustrate that this effect occurred over the entire extent of the Caudal Medullary Raphe, we display the respiratory parameters at baseline (black), after injections into the area caudal to the preBötC level (green), at the preBötC level (brown), and rostral to the preBötC level (red). Statistical comparisons were performed solely between baseline and the values at the end of the injection sequence (red) for naloxone and CTAP, and between the last CTAP injection and end of the naltrindole injection sequence for naltrindole. Wilcoxon-signed-rank test, critical $P=0.017$.

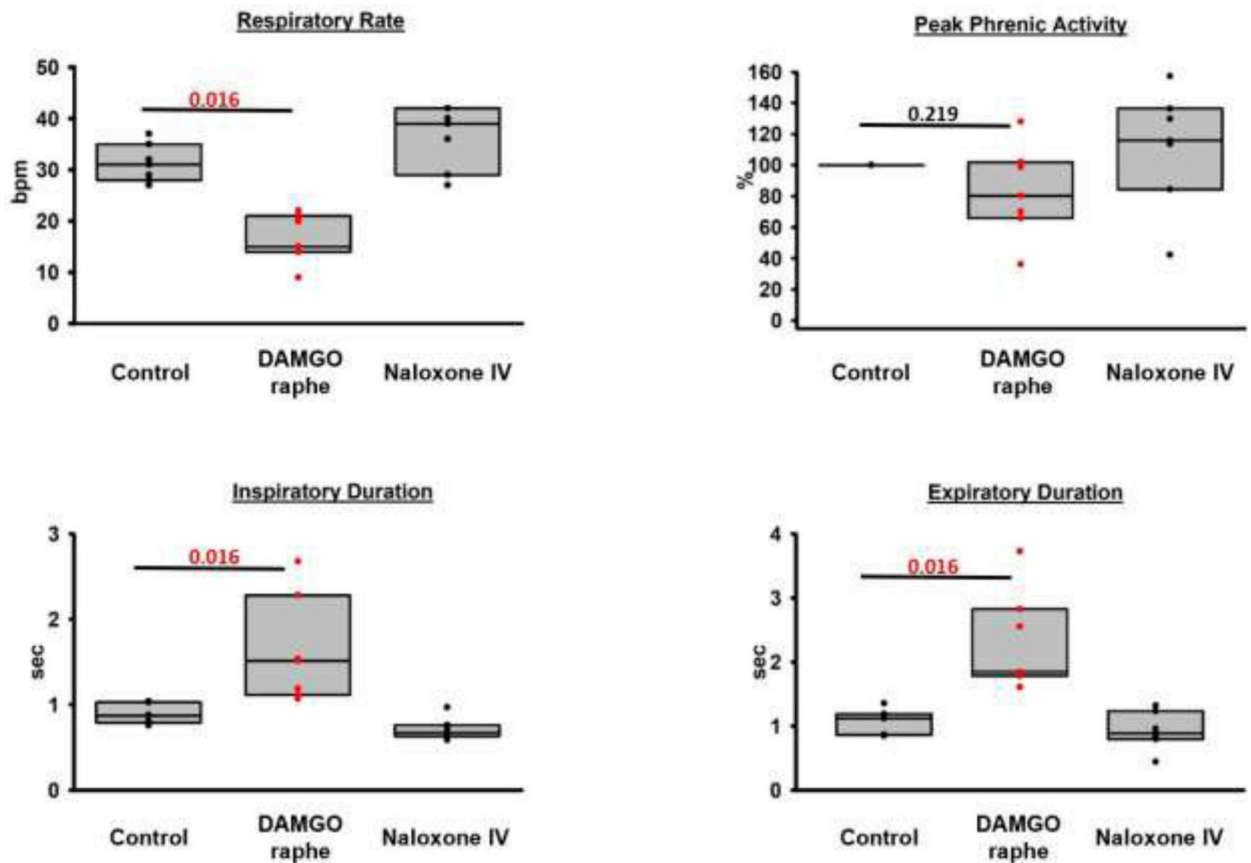


Figure 8:

Pooled data for injections of the mu-opioid receptor agonist DAMGO into the caudal medullary raphe in seven animals. DAMGO depressed respiratory rate through an increase in inspiratory and expiratory phase duration. The effect was reversed by intravenous (IV) naloxone. This shows that endogenous opioids cause only submaximal receptor activation in the raphe. Wilcoxon-signed-rank test, critical $P < 0.05$.

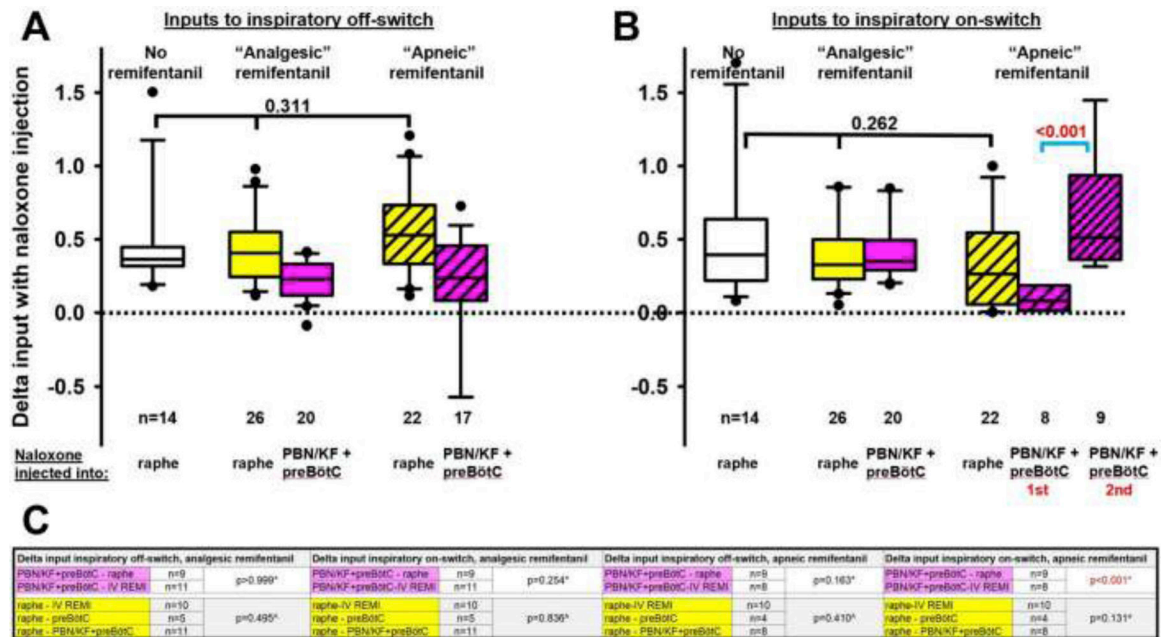


Figure 9: Pooled data for the changes (delta) in inputs to (A) the inspiratory off-switch (derived from the inspiratory duration) and (B) inspiratory on-switch (derived from the expiratory duration) with naloxone injections into the Caudal Medullary Raphe (raphe) or the respiratory rhythm generator, i.e., the Parabrachial Nucleus/Kölliker Fuse Complex (PBN/KF) plus preBötzingner Complex (preBötC). Deltas are compared between naloxone injections without remifentanyl infusion (data from section 3.4., white boxes) or at “analgesic” (section 3.1.) or “apneic” systemic remifentanyl concentrations (section 3.2.). Deltas from different cohorts (naloxone injection orders) were pooled for matching injections (same location and remifentanyl concentration) when they were not statistically different. Comparison of inputs to inspiratory off- and on-switch showed no difference between naloxone injections at different remifentanyl concentrations (black bracket). C: Statistical comparisons between deltas from different cohorts for matching injections (see above) mostly showed no significant differences, and data were thus pooled and used for the analyses in A and B. Inputs to inspiratory on-switch during “apneic” remifentanyl concentrations increased more with naloxone injection into the PBN/KF+preBötC after prior naloxone injection into the raphe and are displayed separately (B, blue bracket, p<0.001). *: Mann-Whitney-U test for two comparisons, ^: Kruskal-Wallis test for three comparisons.

Table 1:

Summary data (median, 25–75% range) for “analgesic” remifentanyl concentrations. Data are presented separately for the different orders of naloxone injection (Cohort A-C). The levels of significance for each comparison are shown in fig.4.

Cohort A: “analgesic” remifentanyl concentration, naloxone injection into the Parabrachial Nucleus/ Kölliker-Fuse Complex, preBötzing Complex, and Caudal Medullary Raphe						
	Control	IV remifentanyl	Naloxone PBN/KF	Naloxone PBN/KF + preBötC	Naloxone PBN/KF + preBötC + CMR	IV Naloxone
Number of animals	11	11	11	11	11	11
Respiratory rate (breaths per minute)	31 (30–36)	16 (15–17)	22 (19–25)	28 (26–33)	36 (34–41)	41 (39–44)
Inspiratory duration (sec)	0.8 (0.7–0.9)	1.4 (1.3–1.6)	1.2 (1.0–1.4)	0.9 (0.9–1.1)	0.8 (0.7–0.9)	0.7 (0.6–0.8)
Expiratory duration (sec)	1.1 (0.9–1.2)	2.5 (2.1–2.8)	1.8 (1.3–1.8)	1.3 (1.0–1.3)	0.9 (0.8–1.0)	0.8 (0.7–0.9)
Peak phrenic activity (%)	100	86 (78–89)	91 (85–101)	95 (88–118)	96 (84–125)	119 (107–154)
Input to inspiratory off-switch [^]	1.8 (1.7–1.9)	1.3 (1.3–1.4)	1.4 (1.3–1.6)	1.7 (1.5–1.7)	2.0 (2.0–2.5)	2.0 (1.9–2.3)
Input to inspiratory on-switch [^]	1.5 (1.5–1.7)	1.1 (1.1–1.1)	1.2 (1.2–1.4)	1.4 (1.4–1.6)	1.7 (1.6–1.9)	1.9 (1.7–2.0)
Cohort B: “analgesic” remifentanyl concentration, naloxone injection into the Caudal Medullary Raphe, preBötzing Complex, and Parabrachial Nucleus/ Kölliker-Fuse Complex						
	Control	IV remifentanyl	Naloxone CMR	Naloxone CMR + preBötC	Naloxone CMR + preBötC + PBN/KF	IV Naloxone
Number of animals	10	10	10	10	10	10
Respiratory rate (breaths per minute)	36 (28–42)	18 (14–20)	35 (28–40)	40 (30–48)	43 (34–52)	45 (40–53)
Inspiratory duration (sec)	0.8 (0.8–0.9)	1.3 (1.1–1.4)	0.7 (0.7–1.0)	0.7 (0.6–0.9)	0.7 (0.6–0.8)	0.6 (0.6–0.7)
Expiratory duration (sec)	0.9 (0.7–1.3)	2.2 (1.8–2.8)	1.0 (0.9–1.2)	0.8 (0.6–1.1)	0.8 (0.6–1.0)	0.7 (0.6–0.8)
Peak phrenic activity (%)	100	92 (89–93)	104 (98–113)	111 (106–122)	113 (109–117)	127 (108–138)
Input to inspiratory off-switch [^]	1.8 (1.6–1.9)	1.4 (1.3–1.5)	2.0 (1.6–2.1)	2.1 (1.6–2.2)	2.1 (1.8–2.3)	2.1 (2.0–2.3)
Input to inspiratory on-switch [^]	1.6 (1.3–1.9)	1.1 (1.1–1.2)	1.5 (1.4–1.7)	1.8 (1.5–2.1)	1.9 (1.6–2.3)	2.0 (1.8–2.3)
Cohort C: “analgesic” remifentanyl concentration, naloxone injection into the preBötzing Complex and Caudal Medullary Raphe						
	Control	IV remifentanyl		Naloxone preBötC	Naloxone preBötC + CMR	IV Naloxone
Number of animals	5	5		5	5	5
Respiratory rate (breaths per minute)	34 (28–36)	17 (14–19)		27 (26–32)	33 (28–43)	40 (32–48)
Inspiratory duration (sec)	0.8 (0.8–0.8)	1.2 (1.1–1.3)		0.9 (0.9–1.0)	0.8 (0.6–0.8)	0.7 (0.5–0.8)

Expiratory duration (sec)	1.0 (0.8–1.3)	2.4 (2.0–2.8)		1.3 (1.0–1.4)	1.0 (0.8–1.4)	0.7 (0.7–1.2)
Peak phrenic activity (%)	100	97 (86–101)		107 (92–127)	108 (91–112)	94 (93–114)
Input to inspiratory off-switch[^]	1.8 (1.8–1.9)	1.4 (1.4–1.5)		1.7 (1.6–1.7)	1.8 (1.8–2.3)	2.0 (1.9–2.4)
Input to inspiratory on-switch[^]	1.6 (1.4–1.8)	1.1 (1.1–1.2)		1.4 (1.3–1.6)	1.6 (1.3–1.8)	1.9 (1.5–2.0)

[^] Values are relative to the threshold for phase-switch, which is set at 1 in our model. IV: intravenous, PBN/KF: Parabrachial Nucleus/Kölliker-Fuse Complex, preBötC: preBötzinger Complex, CMR: Caudal Medullary Raphe.

Author Manuscript

Author Manuscript

Author Manuscript

Author Manuscript

Table 2:

Summary data (median, 25–75% range) for “apneic” remifentanyl concentrations. Data are presented separately for the different orders of naloxone injection (Cohort A-C). The levels of significance for each comparison are shown in fig.5.

Cohort A: “apneic” remifentanyl concentration, naloxone injection into the Parabrachial Nucleus/ Kölliker-Fuse complex, preBötzing Complex, and Caudal Medullary Raphe				
	Control	IV remifentanyl	Naloxone PBN/KF + preBötC	Naloxone PBN/KF + preBötC + CMR
Number of animals	10	10	8	10
Respiratory rate (breaths per minute)	33 (30–36)	0	21 (13–23)	34 (31–41)
Inspiratory duration (sec)	0.8 (0.7–0.9)	2.6 (2.1–3.2)	1.4 (1.1–1.6)	0.8 (0.7–0.9)
Expiratory duration (sec)	1.0 (0.9–1.1)	16.0 (12.2–19.0)	1.7 (1.3–3.2)	0.9 (0.8–1.0)
Peak phrenic activity (%)	100	54 (44–62)	77 (66–88)	87 (73–113)
Input to inspiratory off-switch[^]	1.8 (1.7–2.0)	1.1 (1.0–1.1)	1.3 (1.3–1.5)	1.8 (1.7–2.0)
Input to inspiratory on-switch[^]	1.5 (1.5–1.7)	1 (1–1)	1.2 (1.2–1.3)	1.6 (1.5–1.8)
Cohort B: “apneic” remifentanyl concentration, naloxone injection into the Caudal Medullary Raphe, Parabrachial Nucleus/ Kölliker-Fuse complex, and preBötzing Complex				
	Control	IV remifentanyl	Naloxone CMR	Naloxone CMR + preBötC + PBN/KF
Number of animals	10	10	10	9
Respiratory rate (breaths per minute)	36 (28–42)	0	18 (11–25)	43 (31–48)
Inspiratory duration (sec)	0.8 (0.8–0.9)	2.5 (1.8–3.5)	0.9 (0.8–1.5)	0.7 (0.6–0.9)
Expiratory duration (sec)	0.9 (0.7–1.3)	14.7 (12.7–18.4)	2.6 (1.6–3.9)	0.8 (0.6–1.1)
Peak phrenic activity (%)	100	66 (49–72)	87 (76–99)	94 (89–105)
Input to inspiratory off-switch[^]	1.9 (1.7–1.9)	1.1 (1.0–1.2)	1.6 (1.3–1.9)	2.0 (1.7–2.1)
Input to inspiratory on-switch[^]	1.7 (1.4–1.9)	1 (1–1)	1.1 (1.0–1.3)	1.9 (1.5–2.2)
Cohort C: “apneic” remifentanyl concentration, naloxone injection into the preBötzing Complex and Caudal Medullary Raphe				
	Control	IV remifentanyl	Naloxone preBötC	Naloxone preBötC + CMR
Number of animals	5	5	5	4
Respiratory rate (breaths per minute)	34 (28–36)	0	12 (10–15)	26 (15–37)
Inspiratory duration (sec)	0.8 (0.8–0.8)	2.2 (0.8–2.2)	1.5 (1.2–1.7)	0.9 (0.6–1.2)
Expiratory duration (sec)	1.0 (0.8–1.3)	21.2 (9.7–23.6)	3.3 (2.8–4.3)	1.9 (1.3–3.2)
Peak phrenic activity (%)	100	91 (60–97)	117 (97–148)	116 (106–123)
Input to inspiratory off-switch[^]	1.8 (1.8–1.9)	1.1 (1.1–1.8)	1.3 (1.2–1.4)	1.8 (1.5–2.2)
Input to inspiratory on-switch[^]	1.6 (1.4–1.8)	1 (1–1)	1.0 (1.0–1.1)	1.2 (1.1–1.4)

[^] Values are relative to the threshold for phase-switch, which is set at 1 in our model. IV: intravenous, PBN/KF: Parabrachial Nucleus/Kölliker-Fuse Complex, preBötC: preBötzing Complex, CMR: Caudal Medullary Raphe.